

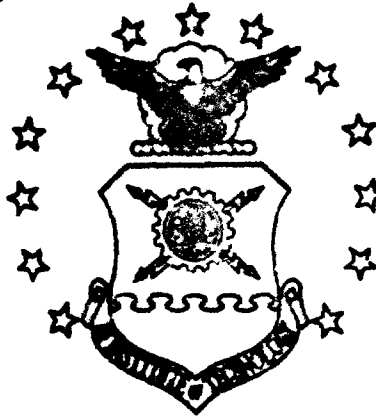
UNCLASSIFIED

AD NUMBER
AD818369
NEW LIMITATION CHANGE
TO Approved for public release, distribution unlimited
FROM Distribution authorized to U.S. Gov't. agencies and their contractors; Operational and administrative use; Jun 1967. Other requests shall be referred to Dean, School of Engineering [AFIF/SE], Wright-Patterson AFB, OH, 45433.
AUTHORITY
AFIT ltr, 22 Jul 1971

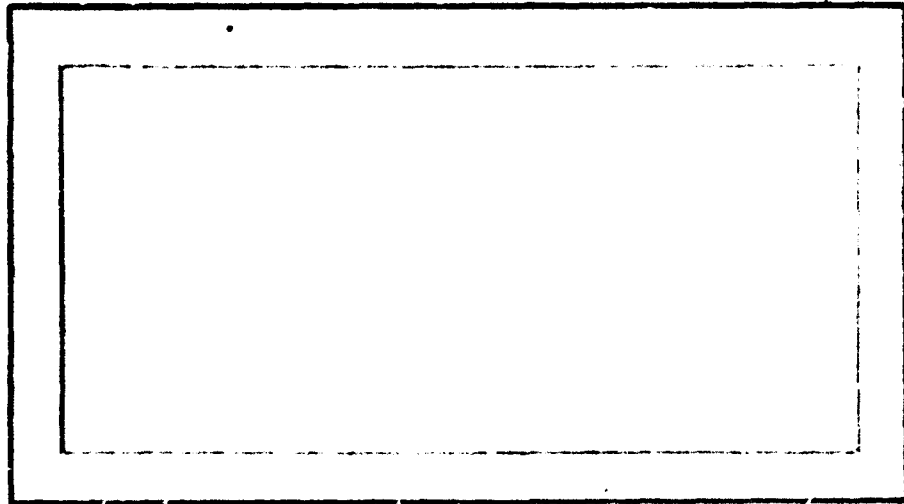
THIS PAGE IS UNCLASSIFIED

AD818369

AIR FORCE INSTITUTE OF TECHNOLOGY



AIR UNIVERSITY
UNITED STATES AIR FORCE



SCHOOL OF ENGINEERING

WRIGHT-PATT AIR FORCE BASE, OHIO

D D C
RECEIVED
AUG 15 1967
RECEIVED

**DIFFERENTIAL SCANNING CALORIMETRY METHODS
IN THE DETERMINATION OF
THERMAL PROPERTIES OF EXPLOSIVES**

THESIS

GAW/MK/67B-3

**Jerry Dean Wilcox
1st Lt USAF**

**THIS DOCUMENT IS SUBJECT TO SPECIAL EXPORT
CONTROLS AND EACH TRANSMITTAL TO FOREIGN
GOVERNMENTS OR FOREIGN NATIONALS MAY BE
MADE ONLY WITH PRIOR APPROVAL OF THE DEAN,
SCHOOL OF ENGINEERING, (AFIT-SE),
WRIGHT-PATTERSON AIR FORCE BASE, OHIO 45433.**

**DIFFERENTIAL SCANNING CALORIMETRY METHODS
IN THE DETERMINATION OF
THERMAL PROPERTIES OF EXPLOSIVES**

THESIS

**Presented to the Faculty of the School of Engineering of
the Air Force Institute of Technology
Air University
in Partial Fulfillment of the
Requirements for the Degree of
Master of Science**

by

Jerry D. Wilcox, B.S.

1st Lt USAF

Graduate Aeronautical Engineering

Air Weapons

June 1967

Preface

This report is an account of my efforts to verify the applicability of the differential scanning calorimeter in determining properties of organic explosives. The work will, hopefully, be a useful guide to gaining further understanding of the behavior of explosives in increasing temperature environments.

The organic explosives used in this study were as received; no attempts were made to purify them or alter their crystalline form. Only those known as "high explosives" were tested. Inorganic explosives such as lead azide were not studied because their higher sensitivity would have made necessary an entirely different laboratory procedure. Amounts of explosives kept on hand were small enough to permit sample preparation and storage with very little danger of injury. Sample sizes were on the order of 1 mg for heat of fusion, purity, and activation energy tests; specific heat test samples were larger -- about 30 mg -- to compare in mass to the test standard used. No laboratory accidents occurred during the test program.

My inspiration for this study was provided by Dr. William C. Bahr, a man with an inquiring mind and a love for research. He motivated in his students an interest in thermochemistry in general and in organic explosives in particular, as well as a lively respect for the technical literature. His sudden death in March removed from our midst a man whose contributions were only beginning, but who may at last be finding some of the answers he continually sought.

I wish to express thanks to Colonel Joseph R. O'Brien, Chief, Weapons Technology Branch, for his assistance in our obtaining the use

of DSC equipment purchased by his organization. Without this special help, the study would not have been possible.

The interest and assistance of Mr. William W. Baker is gratefully acknowledged. His help in setting up the instrument for many of the test runs saved many hours.

Finally, my wife Gloria's helpfulness and serene patience while this study was in progress are greatly appreciated.

Jerry D. Wilcox

Contents

	Page
Preface.....	ii
List of Figures.....	vi
List of Symbols and Subscripts.....	viii
Abstract.....	x
I. Introduction.....	1
Experimental Approach.....	2
II. Apparatus.....	3
Differential Scanning Calorimeter.....	3
Potentiometer Recorder.....	6
Electrobalance.....	6
III. Experimental Procedures.....	7
Preparation of Samples.....	7
Signature Thermograms.....	9
Heat of Fusion Test.....	10
Purity Test.....	10
Specific Heat Test.....	11
Activation Energy Test.....	12
IV. Data Analysis.....	13
Heat of Fusion.....	13
Purity.....	13
Specific Heat.....	15
Activation Energy.....	15
Temperature Correction.....	16
V. Results and Discussion.....	17
Heat of Fusion and Purity.....	17
Factors Impairing Results for TNR, HMX, and RDX.....	17
Causes of Error.....	19
Specific Heat.....	21
Activation Energy.....	23
VI. Conclusions.....	25
VII. Recommendations.....	26
Bibliography.....	27

Figure		Page
B-9	Purity: PETN (3).....	46
C-1	Specific Heat: Sapphire Standard and Empty Cup.....	48
C-2	Specific Heat: TNR, Segmented Scans (Results Only)....	49
C-3	Specific Heat: TNT, Continuous and Segmented Scans....	50
C-4	Specific Heat: Tetryl, Continuous and Segmented Scans.	51
C-5	Specific Heat: HMX, Continuous and Segmented Scans....	52
C-6	Specific Heat: RDX, Continuous and Segmented Scans....	53
C-7	Specific Heat: RDX, Segmented Scans Paste-Up.....	54
C-8	Specific Heat: PETN, Continuous and Segmented Scans...	55
D-1	Activation Energy: Tetryl (1).....	57
D-2	Activation Energy: Tetryl (2).....	58
D-3	Activation Energy: HMX (1).....	59
D-4	Activation Energy: HMX (2).....	60
D-5	Activation Energy: RDX (1) With Data Adjustment.....	61
D-6	Activation Energy: RDX (2) With Two Slopes.....	62
D-7	Activation Energy: PETN (1).....	63
D-8	Activation Energy: PETN (2) No Linearity.....	64
D-9	Activation Energy: PETN (3).....	65
D-10	Activation Energy: PETN (4).....	66

List of Symbols and Subscripts

<u>Symbol</u>	<u>Quantity</u>	<u>Unit</u>
A	Area	arbitrary number
A [*]	Arrhenius frequency factor	1/sec
a	Partial area	same as A
c	Area correction	same as A
Ch	Chart speed	inch/min
C _p	Specific Heat	cal/gm °K
d	Distance measured from interpolated baseline to recorder trace	inches
E [*]	Activation energy	kcal/mole
F	Area fraction	
H _f	Heat of fusion	cal/mole/cal/gm
k	Arrhenius rate constant	1/sec
m	Slope	
q	Heat input	cal
R	Universal gas constant	kcal/mole °K
Ra	DSC range setting	mcal
Sc	DSC scanning speed setting	°K/min
T	Temperature	°K
T _m	Impure melting point	°K
T _o	Pure melting point	°K
w	Weight	mg
X	Mole fraction of impurity	mole

Subscripts

c Area correction c added

Subscripts

- i Successive readings of d or T
- o Original conditions
- p Empty sample pan
- r Reference
- s Sample

Abstract

Differential Scanning Calorimetry methods are applied in determining heat of fusion, purity, specific heat, and activation energy of decomposition for undiluted, unmixed samples of the high explosives TNR, TNT, tetryl, HMX, RDX, and PETN. Thermograms describing energy absorption or evolution from 300°K to 600°K are presented. Heat of fusion and purity results are consistent for explosives which melt at lower temperatures without vaporization, such as TNT and tetryl. Specific heat values in the 313°K to 423°K range all lie between 0.25 and 0.35 cal/gm °K, monotonically increasing with temperature. Activation energies obtained are 20% - 50% higher than those reported from isothermal tests.

DIFFERENTIAL SCANNING CALORIMETRY METHODS
IN THE DETERMINATION OF
THERMAL PROPERTIES OF EXPLOSIVES

I. Introduction

The thermal analysis of organic explosives has for many years yielded information to improve the design and safe manufacturing procedures of weapons and related devices. One useful technique has been differential thermal analysis (DTA), in which the temperature of a sample is compared with the temperature of a reference material while both are being heated at some controlled temperature rate. The results are usually plotted as temperature difference versus reference temperature. The differential scanning calorimeter, developed by the Perkin-Elmer Corporation in 1963, combines the DTA method of temperature comparison with closed loop heat addition. Rather than difference in temperature, the quantity measured by this instrument is the electrical power in calories per second required to maintain the sample and reference at the same temperature. Thus, the actual power supplied to either the sample side -- in an endothermic reaction such as melting, or the reference side -- in an exothermic reaction such as decomposition, is plotted on the recorder chart versus temperature. The recorder output shows endothermic and exothermic peaks whose areas are directly proportional to the energy absorbed or liberated by the sample. This feature suggests that quantitative studies of reactions involving energy change are possible. The purpose of this study, then, is to investigate the applicability of differential scanning

calorimetry techniques to the determination of thermal properties of explosives.

Experimental Approach

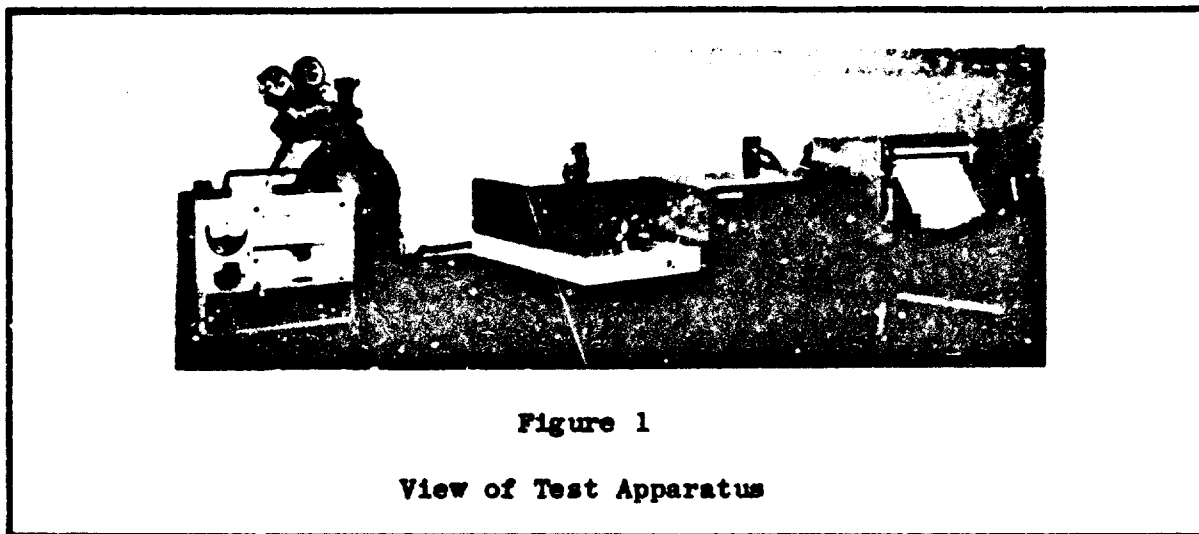
The use of the differential scanning calorimeter in determining heat of fusion, purity, specific heat, and activation energy for decomposition was investigated for the following explosives: TNR, TNT, tetryl, HMX, RDX, and PETN. Magnified (3.75X) views of the actual explosives used are given in Figure 6.

The following experimental procedures were applied:

1. Heat of fusion was calculated by comparing the area of the sample's melting endotherm with the area of indium's melting endotherm.
2. Purity determinations were made by comparing the shape and curvature of the sample's melting endotherm with the shape and curvature of a pure sample of indium metal.
3. Specific heats were determined by directly comparing the recorder trace displacements of the sample with those of a reference material at successive temperatures.
4. Activation energy was determined by studying the shape and curvature of the leading edge of the decomposition exotherm.

II. Apparatus

The equipment used in this study consisted of a Perkin-Elmer Model DSC-1B Differential Scanning Calorimeter and accessories, Leeds and Northrup "Speedomax W" Potentiometer Recorder, and a Cahn Gram Electrobalance, Model G. These instruments are shown in Figure 1.



Differential Scanning Calorimeter

Figure 2 shows the differential scanning calorimeter, Perkin-Elmer Cat. No. 219-0139, which consists of a sample holder assembly, transparent-top sample enclosure cover, sample holder base unit, and control unit. The removable sample holder assembly, Figure 3, consists of a base plate upon which two 0.27 inch inside diameter sample holders are symmetrically mounted with platinum resistance thermometers and heating elements embedded in the base of each, and with purge gas inlet and outlet tubes extending downward into the base unit. The sample enclosure cover has two ports whose teflon stoppers can be removed for access to the sample holders during use. The control unit contains a multi-range two-directional linear temperature programmer with eight scan speeds from 0.625 °K/min to 80 °K/min, a range sensitivity

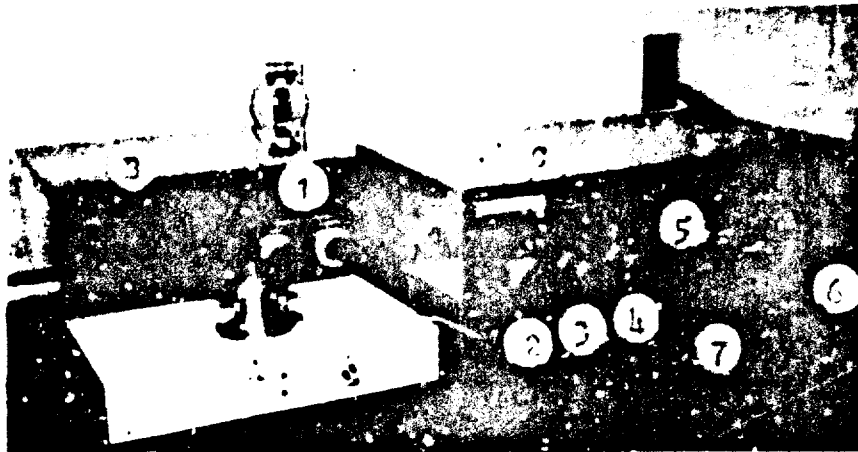


Figure 2

Differential Scanning Calorimeter

- | | | | |
|---|-------------------------|---|-------------------------|
| A | Sample Holder Assembly | 3 | Range Selection |
| B | Base Unit | 4 | Trace Pen Zero |
| C | Control Unit | 5 | Scan Speed Selection |
| 1 | Temperature Calibration | 6 | Temperature Programming |
| 2 | Slope Adjustment | 7 | Scan Increase, Decrease |

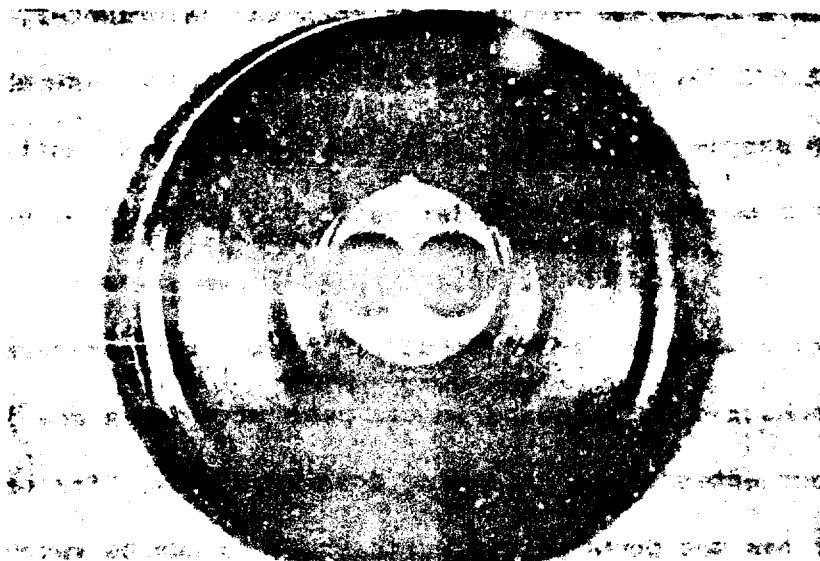


Figure 3

Closeup of Sample Holder

selector with seven ranges from 1 to 64 millicalories full scale, transistorized amplifiers and power supply, and electronic baseline slope compensator. Normal temperature range is 273°K to 773°K . Accessories include a Sola type CVS constant voltage transformer (not shown) and a nitrogen purge gas system with a filter dryer and a Matheson gas regulator.

The DSC-1B calibration performed at the factory was reported as a chart of suggested settings for the two temperature calibration dials on the base unit. The sample holder for which the calibration had been performed was installed in the base, and the calibration was repeated according to the published instructions for the equipment as installed. Since no deviations in temperature were observed, the suggested settings were used throughout the experimental work. The same sample holder was used for all experiments.

Potentiometer Recorder

The Leeds and Northrup potentiometer recorder, Figure 4, is a downward feed strip chart recorder with a horizontally moving trace pen to record the differential power signal from the DSC-1B sample holder and a second pen at the right margin to mark

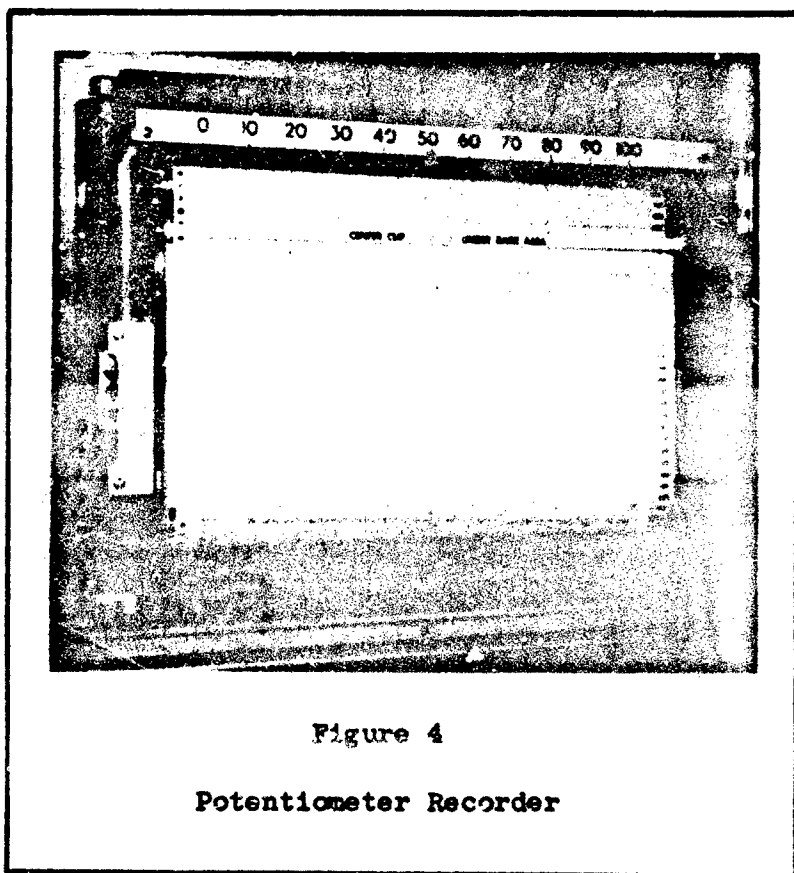


Figure 4

Potentiometer Recorder

each degree of increase or decrease of the temperature programming dial. Three chart speeds are available: 0.25, 1.0, and 4.0 inches per minute.

Electrobalance

The Cahn Gram Electrobalance, Figure 5, has eight selected full-scale ranges from 0-1 to 0-1000 milligrams, with a precision of 0.0001 mg on the smallest scale. Accessories include a set of calibrating

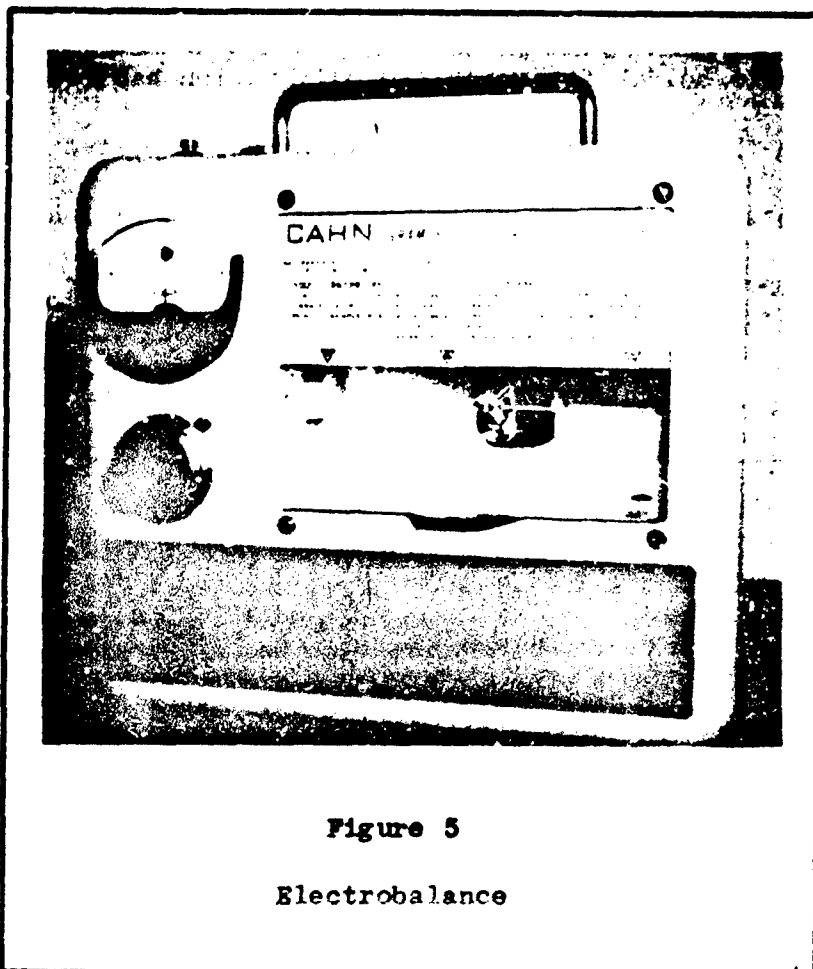


Figure 5
Electrobalance

weights, forceps, and two sizes of weighing pans and stirrups. In order to handle gross weights ranging from 20 to 60 mg, the 0-100 mg scale was used in this study. The precision on this range, given as 0.01 mg, was verified by exact duplication of weighings over a period of several weeks.

III. Experimental Procedures

Many methods have been developed by DSC users to take advantage of the instrument's capability for quantitative energy determinations. Sources for the four tests described in this report are as follows: heat of fusion (Ref 8:42), purity (Ref 35:1), specific heat (Ref 20:1331), and activation energy (Ref 28:412).

Full scale recorder deflections for heat of fusion, purity, and activation energy tests were obtained for samples of 1 mg or less, depending on the control settings chosen. Four DSC control settings were available: range (Ra) in millicalories full scale, scan speed (Sc) in Kelvin degrees per minute, chart speed (Ch) in inches per minute, and slope, dimensionless. The Ra setting provided ordinate size control, while Sc and Ch gave abscissa control. To facilitate comparison, most tests of a series were run with similar settings.

In all tests with the DSC, a straight baseline parallel to the recorder chart edges was sought. Depending on the results of the first try with an "average" setting, the slope control was adjusted up or down until a straightness adequate for the test to be performed was achieved. The effect of slope setting on recorded areas was assumed negligible for tests having a baseline within a few degrees of parallel to the chart edges.

Preparation of Samples

In the preparation of a sample, Figure 7, a small amount of explosive (stock described in Figure 6) was removed from the storage vial and placed in an aluminum cup of 1/4 inch diameter, which was placed on the left stirrup of the electrobalance for weighing. The

Figure 6

Details of Explosives Stock

		
1. TNR	2,4,6-trinitroresorcinol $(NO_2)_3C_6H(OH)_2$ pale green-yellow	
2. TNT	2,4,6-trinitrotoluene $(NO_2)_3C_6H_2CH_3$ pale yellow	
3. Tetryl	N-methyl-N,2,4,6-tetranitro- aniline $(NO_2)_3CH_3NNO_2$ yellow	
4. HMX	Octahydro-1,3,5,7-tetranitro- 1,3,5,7-tetrazocine $(NO_2)_4N_4(CH_2)_4$ white	
5. RDX	1,3,5-trinitro-s-triazine $(NO_2)_3N_3(CH_2)_3$ pale tan	
6. PETN	Pentaerythritol tetranitrate $C(CH_2)_4O_4(NO_2)_4$ white	

net sample weight was then obtained by subtracting the pre-recorded tare weight of the pan and its flat aluminum lid.

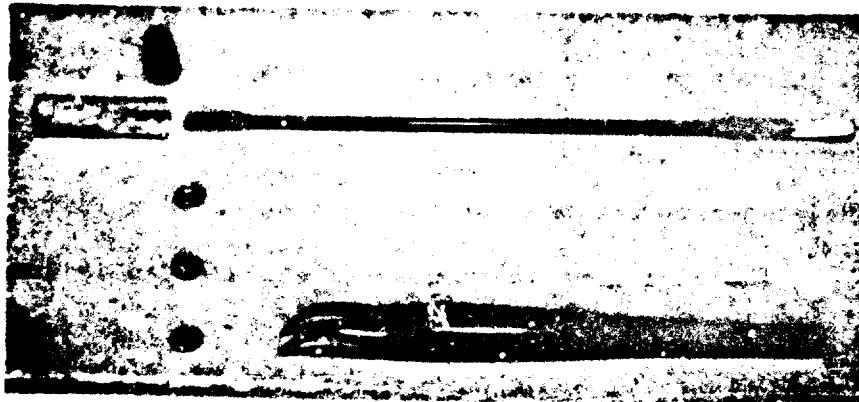


Figure 7

Sample Preparation

The sample pan edges could then be rolled downward over the pan lid by use of the special crimping press, a DSC accessory. Crimped samples were less likely to be spilled in handling or storage. Activation energy test samples were crimped, as were those for the signature thermograms. However, the crimping process frequently caused the bottom surface of a sample pan to bulge inward, reducing the area for thermal conduction from the sample holder to only the edges of the lower surface. Because the crimped samples displayed varying degrees of bulging, purity tests were run with covered, uncrimped samples to ensure a flat surface of contact. An additional factor for specific heat tests, also uncrimped, was the large size (about 30 mg) required; some samples would have been spilled by the crimping process itself.

Signature Thermograms

Before the primary tests could be run a general knowledge of an explosive's behavior due to rising temperature was necessary. For

this reason, a sample of each explosive was heated at a constant rate (i.e. scanned) from ambient temperature to the point where its thermal activity ended -- between 500^oK and 600^oK. The recorder trace thus produced is called a thermogram. Such thermograms, uniquely describing the thermal behavior of the samples which produced them, are called "signature thermograms" in this report. They were used as guides for selecting the temperature ranges of interest of each explosive for the various tests. The signature thermograms are presented in Appendix A.

Although the convention "endotherm downward (to the right of one facing the recorder) and exotherm upward," as followed in this report, does not conform to recommended DSC practice, it allows direct comparison with the many results of differential thermal analysis tests over the last several years.

Heat of Fusion Test

The latent heat of fusion was determined by measuring the area of the melting endotherm of the sample and comparing it with that of a standard pure material. The 5.95 mg indium (99.9999%) sample provided with the DSC equipment was used as the standard. In this study the heats of fusion were generally calculated as a preliminary step in the purity determinations.

Purity Test

Sample size was adjusted to that which would produce a large melting endotherm at instrument settings of Ra, 2 mcal full scale, Ch, 4 in/min and Sc, 0.825 ^oK/min. The initial temperature was set far enough below the onset of melting shown on the signature thermograms to ensure that the entire visible leading edge was included

in the record. The trace pen was set on the low specific heat (left) side of the recorder chart to allow space for the melting endotherm to form. After the instrument had come to equilibrium -- about two minutes -- the sample was scanned upward through the melting transition. A return baseline was established in each test before stopping the scan.

Specific Heat Test

A flat disc of aluminum oxide (in the form of synthetic sapphire or corundum) provided as an accessory to the DSC instrument was used as a standard reference material for the specific heat tests. The baseline displacement of the sapphire, due to a programmed energy input producing a temperature rise of $10^{\circ}\text{K}/\text{min}$, was compared at ten degree intervals from 313°K to 423°K to that of known weights of explosive. Large enough samples were used to produce specific heat displacements of the same order of magnitude as those of the sapphire. Two dome shaped aluminum sample holder covers fitting snugly over each sample holder were used as radiation shields to minimize thermal emissivity changes of the sample during heating.

Two different types of test series were performed and are compared in this report: (1) two series of six short scans through overlapping segments of the temperature range, and (2) one continuous scan over the entire temperature range. In each test the sapphire, empty pan, and the six samples in turn were scanned through the required range. To allow the scanning baseline to adjust itself, the instrument for each test was equilibrated at 15 degrees below the temperature at which the first reading was desired. The results are

compared graphically in Appendix C.

Activation Energy Test

The rate of energy evolution at any temperature is proportional to the distance between the rising decomposition curve and the interpolated baseline at that temperature. Explosives which vaporize before reaching their decomposition temperature, however, cannot be tested for activation energy by the method used here. Of the six explosives being considered in this report, TNR and TNT are in this category; for each of the other four explosives activation energy determinations were attempted.

With a small (about 1 mg) sample in the sample holder, and the trace pen on the high specific heat side (right) of the recorder chart, the instrument was equilibrated at a temperature below that for which any exothermic deflection was indicated on the explosive's signature thermogram. Each run was performed with Ch, 4 in/min, while Sc and Ra settings were adjusted to the expected exotherm's size and shape. Although for purity determinations the melting peak had to be kept entirely on the chart for area measurement, only the leading edge of the activation energy exotherm had to be preserved. Thus Sc and Ra adjustment to keep the peak entirely on the chart was not critical.

IV. Data Analysis

The raw data from the four types of tests performed in this study consisted of (1) chart recorder traces of DSC power (mcal/sec) versus temperature, with the associated control settings of Ra, Sc, and Ch, and (2) sample weight (mg), where required. Details on the calculation of the heat of fusion, purity, specific heat, and activation energy are presented in this section.

Heat of Fusion

The basis for calculation of heat of fusion by DSC is the instrument's direct measurement of the power input required to hold the temperature difference between sample and reference equal to zero. The endotherm produced during melting is then proportional to the energy absorbed during fusion. To obtain the energy of transition, the area under the endothermic peak and above the interpolated baseline was measured and compared with that of the pure indium standard, whose latent heat of fusion is known to be 6.8 cal/gm. The method is summarized as follows:

$$\frac{(H_f)_{\text{Sample}}}{(H_f)_{\text{Indium}}} = \frac{\left(\frac{A}{w} \frac{Ra}{Ch}\right)_{\text{Sample}}}{\left(\frac{A}{w} \frac{Ra}{Ch}\right)_{\text{Indium}}} \quad (1)$$

Purity

Purity was found from measurements of the increasing area at corresponding temperatures along the melting curve. Temperature points at which partial area measurements were to be made were marked along the interpolated baseline of the endotherm. Then "slope" lines, equal in slope to the leading edge of the indium melting endotherm, were

drawn from these points to the trace, defining points along the trace from which verticals were drawn to the baseline (see melting traces, Figures B-1 to B-9). Thus the boundaries of the partial areas, with their corresponding temperatures, were completely described. The ratio of partial area to total measured area, a/A , was defined as F , the area fraction. Finally, a plot was made of temperature T_g as a function of reciprocal F .

Even though extra efforts were made to obtain a straight and parallel baseline trace before visible melting deflection, the T_g vs $1/F$ plot was not the straight line predicted by the theory (see Appendixes B and F), indicating that not all the energy absorbed in melting was represented by the area between the curve and the interpolated baseline. To correct for this effect the data was modified as suggested in Ref 36:1-4. The plot for

$$(1/F)_0 = A/a \quad (2)$$

was not a straight line; but with

$$(1/F)_c = (A + c)/(a + c) \quad (3)$$

the locus became straight for a specific value of c . This occurred when $(1/F)_c$ values for successive partial areas differed by a constant. The corrected area, $(A + c)$, was used in the heat of fusion determination. Finally, the slope m and intercept T_0 of the modified T_g vs $(1/F)_c$ plot were then used in the equation

$$X = \frac{m H}{R T_0^2} \quad (4)$$

to obtain the fraction of impurity, X , present in the explosive.

Actual thermograms, along with original and corrected data,

plotted points, and calculations, are presented in Appendix B.

Specific Heat

As samples were scanned on the DSC, the increase in specific-heat with increasing temperature was indicated by a deflection of the trace from the established pre-scanning baseline.

At each temperature of interest the total displacements of sapphire reference, empty pan, and sample were measured in inches. The empty pan displacement at each temperature was added to the respective sample and sapphire reference displacements in the following ratio:

$$\frac{C_{p,s}}{C_{p,r}} = \frac{(d_s + d_p)/w_s}{(d_r + d_p)/w_r} \quad (5)$$

where $(d_s + d_p)$ and $(d_r + d_p)$ are the net trace displacements due to the sample and sapphire reference, respectively.

The weight, w_r , of the sapphire reference was found to be 34.34 mg. The values of $C_{p,r}$ for each temperature of interest were obtained from a chart provided with the DSC specific heat standards. Control setting Ra in all tests was 4 mcal full scale.

Activation Energy

The ordinate deflections on the decomposition exotherm corresponding to several successive temperature readings were measured and plotted versus temperature in the form $\log_{10} d_1$ vs $1/T_1$. The plot obtained from these data was a modified Arrhenius plot which differs from the usual only in the use of deflection distance d in place of rate constant k along the ordinate. This modification was done because the distance measured is directly proportional to the rate of

energy evolved, and thus is proportional to the Arrhenius rate constant k . For those tests whose data plots were straight lines, then, the activation energy E^* was calculated by the following equation:

$$-(E^*/R) = \frac{2.303 (\log_{10}d_1 - \log_{10}d_2)}{1/T_1 - 1/T_2} \quad (6)$$

or

$$E^* = \frac{-4.58 \log_{10}(d_1/d_2)}{1/T_1 - 1/T_2} \quad (7)$$

The development of equation (7) is given in Appendix G.

Actual decomposition exotherms, along with measured data, plotted points, and calculations, are presented in Appendix D.

Temperature Correction

The temperature readings from the DSC temperature programming dial were not exactly correct. The indium and tin samples provided with the DSC instrument melted at 429.03°K and 506.83°K, according to the dial. This compares with the actual melting points of 429.6°K and 504.9°K, respectively, resulting in differences of -0.57°K for indium and +1.93°K for tin. In examining the results of representative tests to determine the effect of this correction, it was found that a -2.0°K temperature correction in the RDX result for E^* resulted in a negative adjustment of 0.6 kcal/mole, or 0.83%. Since other corrections would have been less, no general temperature correction was made.

V. Results and Discussion

The calculated results for each of the properties considered in this study are presented in Figures 8 - 11, along with comparisons with results published in the literature.

Heat of Fusion and Purity

Of the six explosives considered, only TNT, tetryl, and PETN were tested successfully for purity and heat of fusion by the DSC method. Results are given in Figures 8 and 9. The other three explosives presented various problems, some of which are described in this section.

Very little data for comparison with the purity results was available; only HMX and PETN values were found (see Appendix E). The PETN stock from which all DSC samples were drawn was described as "at least 98% pure"; the lowest purity indicated by these test results was 99.14%. Purity of HMX was quoted as 99.8%; unfortunately this could not be verified by the DSC methods.

Factors Impairing Results for TNR, HMX, and RDX. The TNR results were impaired by the occurrence of (a) endothermic changes at twelve and five degrees below the onset of melting (see Figure A-1), and (b) vaporization before melting. As a result, fast scanning (Sc, 5 or more) did not allow time for the recorder trace to form the essential straight baseline between crystallization and melting, while slow scanning magnified sample loss by vaporization.

HMX did not entirely melt before its decomposition began; therefore, the melting area was incomplete for fast scan speeds and non-existent for slow speeds. The HMX signature thermogram (Figure A-4) shows this phenomenon.

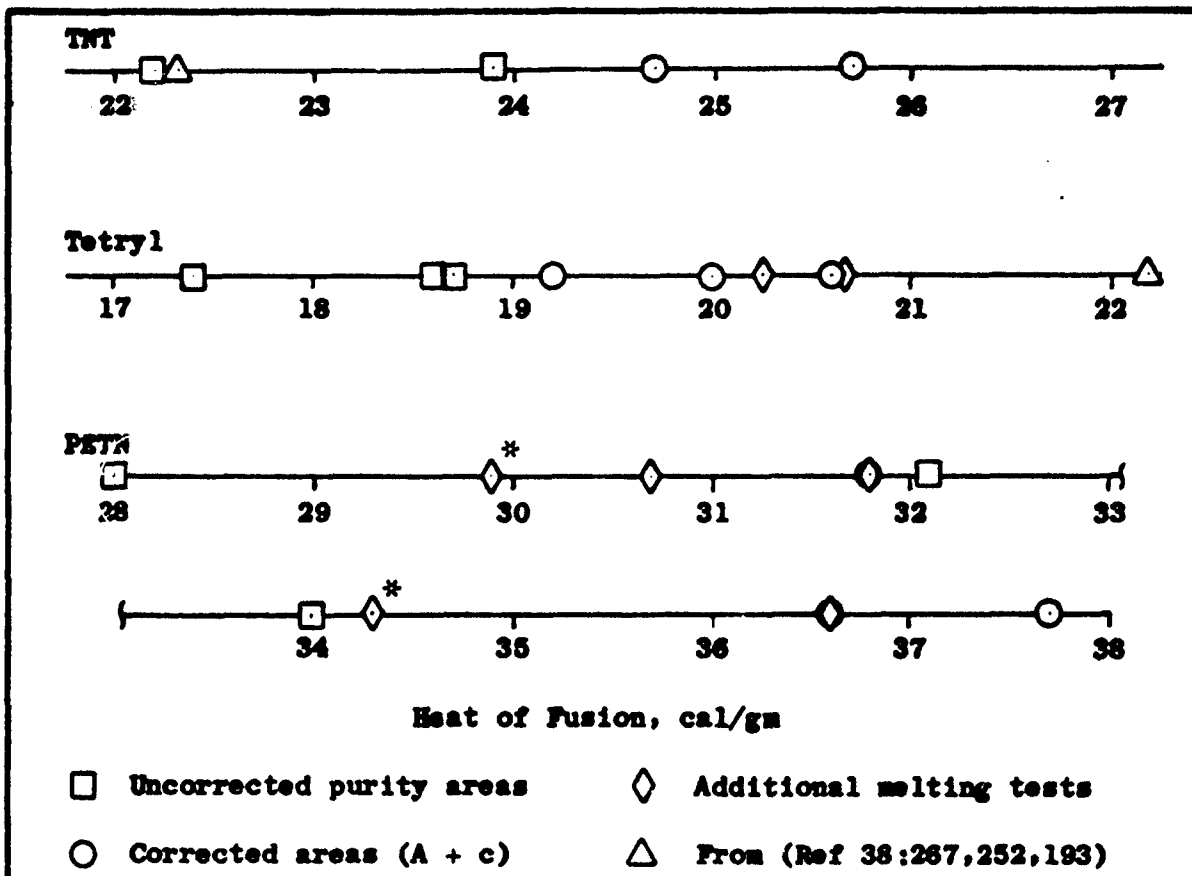


Figure 8
 Comparison of Heat of Fusion Calculations

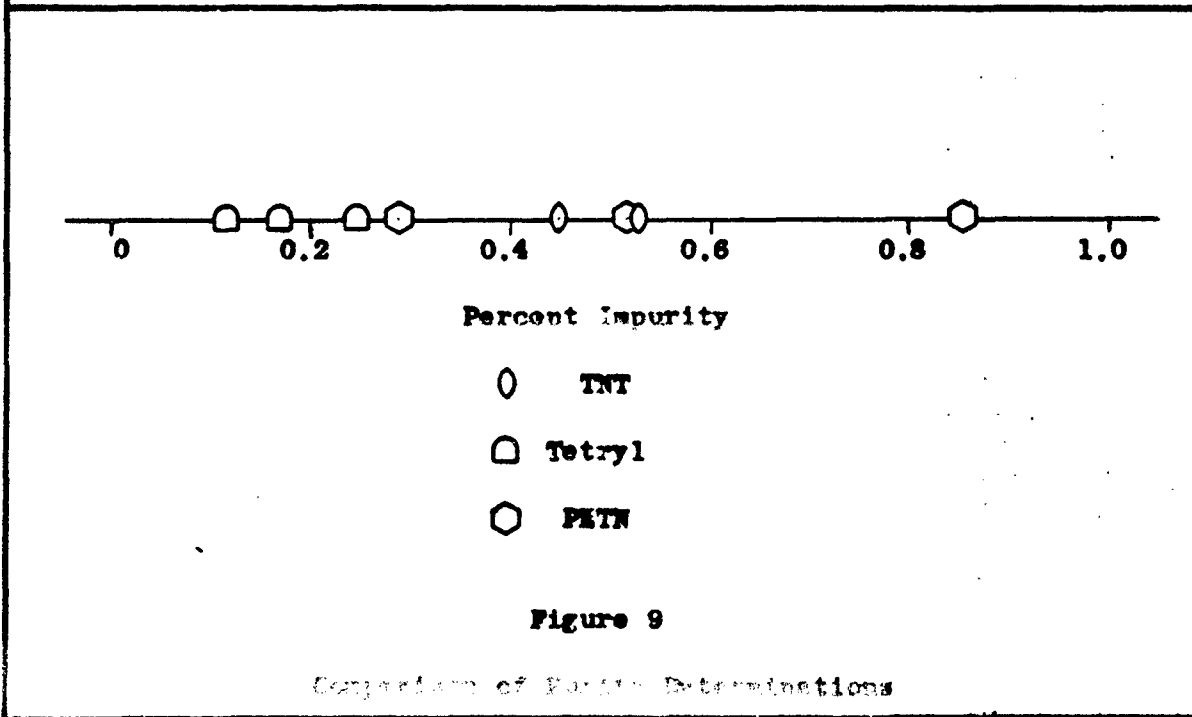


Figure 9
 Comparison of Purity Determinations

The melting of RDX was followed by an upward shift in the trace after melting, as shown on the signature thermogram (Figure A-5). This indicated that sample was being lost by vaporization before the occurrence of decomposition. No RDX melting endotherm could be produced on a slow scan speed (Sc, 0.625); instead, the recorder trace consisted of a series of alternating endo- and exothermic peaks of decreasing amplitude, 20% to 5% of chart width, and centered 4% to the endothermic side of the original baseline. This effect was probably caused by alternating melting and vaporization; no sustained exothermic tendency was observed until at least fifteen degrees above the temperature at which melting had begun.

Causes of Error. Heat of fusion values both with and without the area correction are compared with separate test values in Figure 8, indicating the approximate range of reproducibility attained in these tests. After practice with the planimeter it was observed that the areas could be measured within 1% of average over a series of measurements with several pole positions and starting points. The differences in the results given, showing a variation ranging from 2% for tetryl to 18% for PETN, indicate that factors other than inaccuracy in the mechanical area measurements probably affected the reproducibility of these values.

One step which very likely introduced error was the interpolation of the baseline to the tail of the melting endotherm when the return baseline was not level with the initial baseline. An arbitrary convention was to extend the initial baseline to the point immediately under the peak, then draw a line to the established return baseline. This is shown, for example, in Figure B-7. Results of direct interpolation of

baseline, ignoring the above convention, indicate that the interpolated baseline's location was critical: there was 7% difference between "before" and "after" values, marked with an asterisk (*) in Figure 8.

Another problem was the slight vaporization of some samples before and during melting. Vapor was observed during the melting of PETN, and final weight was consistently 5% to 8% lower than initial weight. Although average weight was used for heat of fusion calculations, the results showed considerable scatter.

Specific Heat

Results in the literature, as plotted for comparison in Figure 10, indicate that specific heat curves have decreasing positive slope with rising temperature. Figure 10 shows that specific heat curves for the explosives tested are monotonic increasing, but only the HMX curve exhibits a tendency toward decreasing slope. The erratic behavior of the TNR and PETN curves may be due in part to weight loss and vaporization observed for both. The averaged curves for TNT, tetryl, and PETN in Figure 10, as well as the continuous scan results in Appendix C, show that at the scanning speed and range sensitivity used (S_c , $10^{\circ}\text{K}/\text{min}$; R_a , 4 mcal) the deflection toward melting began quite early. This tendency, then, may have canceled the expected decrease in slope.

The relative position of the recorder trace pen during scanning was always proportional to two parameters: (1) size of sample, and (2) specific heat, C_p , of sample. If an unchanged zero setting for the trace pen is assumed, the trace produced by a small sample was on the low specific heat side (left) of a larger sample of similar

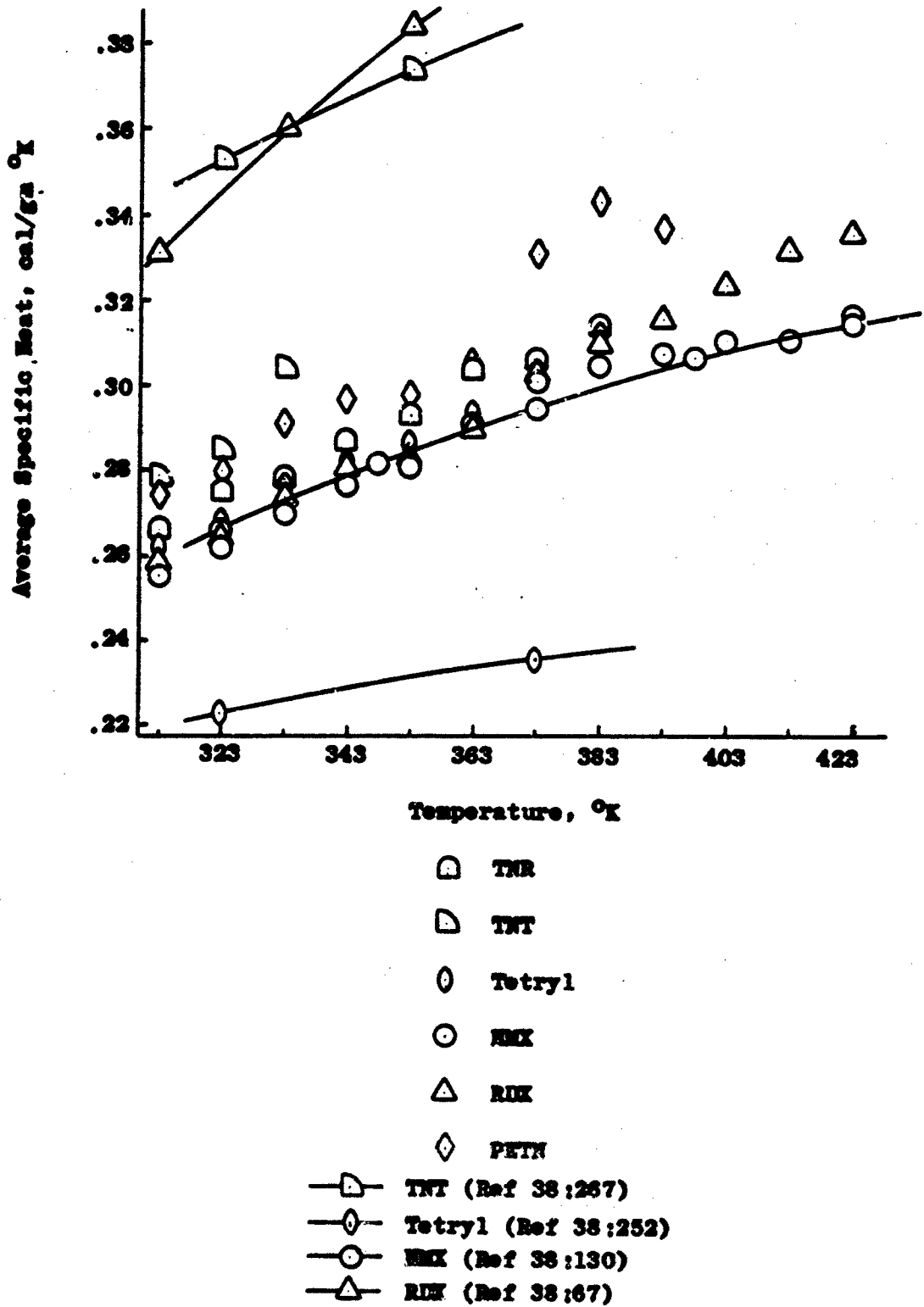


Figure 10

Comparison of Average Specific Heat Values

material; likewise, the trace for a sample with low C_p occurred to the left of that for a higher C_p sample of equal mass.

Although the average C_p curve for HMX matches literature values quite well, no explanation has been found for the wide differences between the TNT, tetryl, and RDX curves and their literature counterparts shown in Figure 10. It is possible that the density and form of the samples for which reference results are reported were quite different from those of the tests in this report. However, although the tetryl sample used in the second C_p test series was the melted and refrozen sample from the first series, the results were very close (see Figure C-4). Therefore the above explanation appears incomplete.

Activation Energy

Calculations by the DSC method yielded comparatively high values of activation energy, E^{\ddagger} , for each explosive. Results for tetryl, RDX, and PETN were 5% higher than those of Ref 28:413, where the same method was used. Figure 11 shows these and other values of E^{\ddagger} .

The return baseline for decomposition exotherms was even less likely than those of purity tests to be found at the pre-reaction chart position. In an attempt to determine the effect of a shifted baseline on the slope of the $\log_{10}d$ vs $1/T$ curve, new baselines were drawn at an arbitrary angle of eight degrees below the original on the tetryl, HMX, and PETN exotherms shown in Figures D-2, D-4, and D-7, and distance versus temperature data was retaken. The tetryl and HMX calculations gave a significantly lower slope, reducing calculated E^{\ddagger} values by 19% in each case. No noticeable improvement could be observed for the PETN data, however. It was concluded that, in general, a baseline

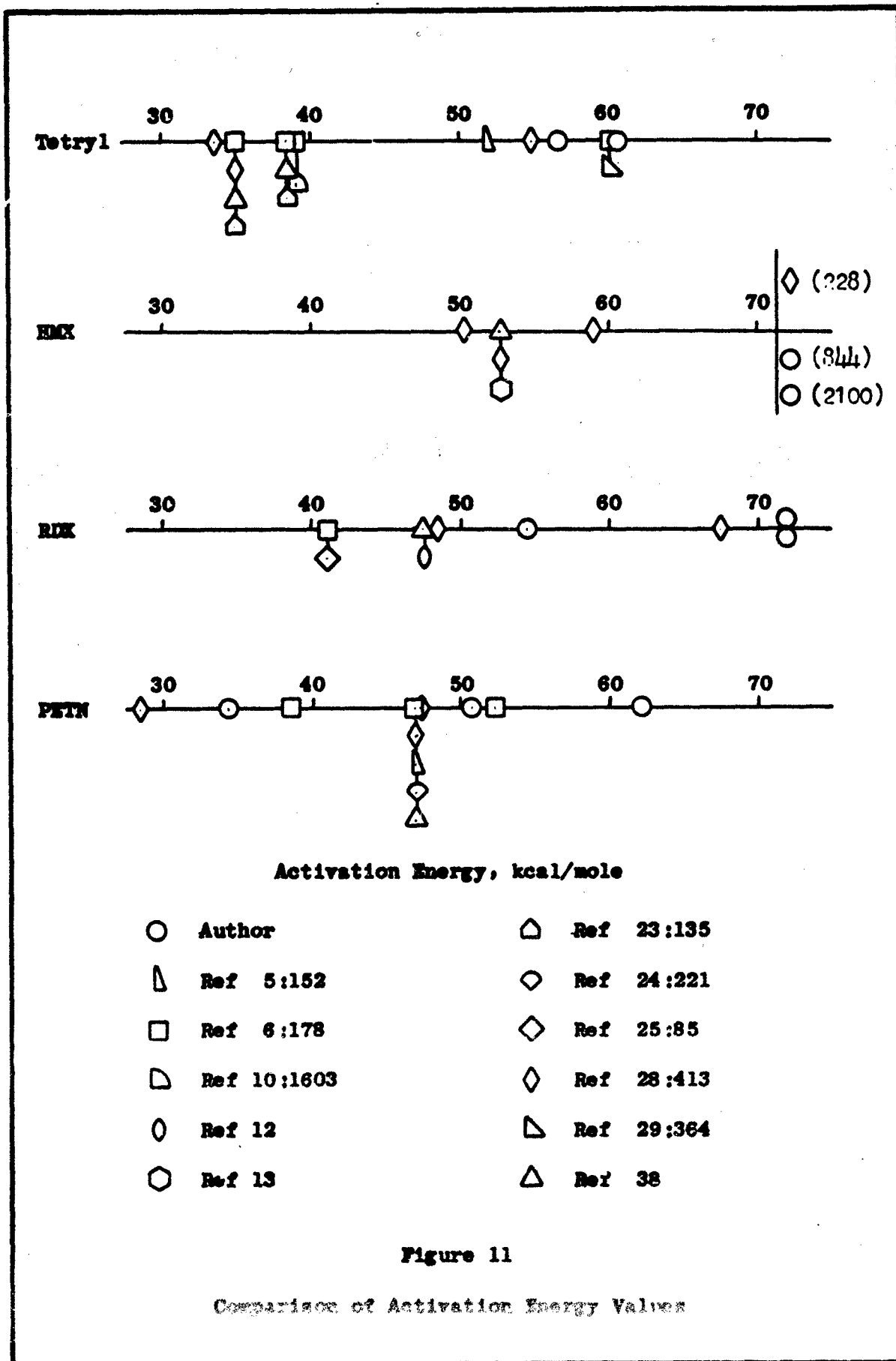


Figure 11

Comparison of Activation Energy Values

extrapolated toward endothermic would yield lower values of E^* . As a matter of convention, then, the pre-decomposition baseline was extended co-linearly, regardless of the location of the return baseline. For either an inert reference material or an empty sample cup the DSC trace usually began increasing in non-linear deflection toward endothermic at a temperature between 500 and 550 °K. This observation strengthens the validity of the above convention.

Many activation energy values presented in literature have resulted from isothermal decomposition tests, in which the explosive sample was by some mechanism placed suddenly in thermal contact with a conducting medium at a specified temperature. By the Arrhenius equation (see Appendix G), since the fraction decomposed after t seconds equals t times k , the plot of $\ln k$ vs $1/T$ for a series of temperatures yields E^*/R as the slope of the line. Results were 20 to 50 percent higher than those of the isothermal tests. Since there are indications that this may severely affect the usefulness of the E^* values (see Ref 33:8), a modification of the DSC method is indicated. For the description of a promising technique using solvents, see Ref 28:413.

Since activation energy is a measure of an explosive's susceptibility to decomposition at any temperature, a high E^* normally indicates slow decomposition. Where design temperatures are critically high, then, an incorrectly high value of E^* would imply rates of decomposition lower than those which would actually be observed. In many applications this could contribute to dangerously premature or accidental decomposition. Thus, with other factors being equal, a calculated value of E^* which is too low would appear to be better than one which is too high.

VI. Conclusions

Based on the results of this study of the applicability of DSC methods to the determination of explosive properties, the following conclusions are drawn:

1. Heat of fusion and purity results are impaired by (a) the presence of vaporization before or during melting, and (b) the occurrence of decomposition near the melting point. Explosives without these problems, such as tetryl and TNT, give consistent results.
2. At temperatures just below the melting range the accuracy of specific heat tests is affected by (a) the beginning of trace deflection due to melting, and (b) sample loss due to vaporization. Explosives with high melting points, such as HMX, give best results.
3. The activation energy values for undiluted explosive samples are high as compared with those from isothermal tests. Modifications making DSC activation energy results more useful appear possible.

VII. Recommendations

It is recommended that homogeneous binary explosive mixtures be tested by the DSC method to determine the extent of variation in the melting point, decomposition temperature, and activation energy of one explosive due to the introduction of increasing mole percentages of another explosive. Such data could be presented in phase diagram form.

It is recommended that DSC methods be used to compare the properties of recently developed explosives such as TFET, PF, and WNTF with similar explosives already in wide military use, both in pure form and in mixtures over a range of percent compositions.

It is further proposed that tests using sealed sample cups (DSC Part No. 219-0062) be performed and their results compared with those presented in this report for open and crimped cups. The sealed cups may make possible more reproducible results for those explosives such as TNR, PETN, RDX, and TNT which showed vaporization before decomposition.

Finally, it is recommended that the heat sensitivity of explosives be studied, with emphasis on determining the induction time at various temperatures at and above the decomposition point. It is suggested that the memory effect, which is the possibility that induction time is shortened by the effects of previous partial heating, be observed and reported.

The necessary equipment and supplies for the recommended studies are available.

Bibliography

1. Andreyev, K. K. "Thermal Decomposition and Combustion in Explosive Materials." Explosivstoffe, 2, 35 (1962). AD 474 121.
2. "Application of Differential Thermal Analysis to Military High Explosives." U.S. Naval Weapons Station. NAVORD Report 5802 (January 1960).
3. Baum, F. A., K. P. Stanyukovich and B. I. Shekhter. Physics of an Explosion (1959). Translated from the Russian by Research Information Service. AD 400 151.
4. Belyaev, A. F. "Mechanism of Thermal Ignition of Explosives" (1946). Translated from the Russian by U. S. Joint Publication Research Service, April 1965. AD 461 152L.
5. Bowden, F. P. and A. D. Yoffe. Fast Reactions in Solids. London: Butterworth Scientific Publications, 1958.
6. Cook, M. A. The Science of High Explosives. New York: Reinhold, 1958.
7. Cook, M. A. and M. T. Abegg. "Isothermal Decomposition of Explosives." Ind and Eng Chem, 48, 1090 (1956).
8. Differential Scanning Calorimeter Instructions, November 1966. Perkin-Elmer Corporation, Norwalk, Connecticut.
9. Dubiel, S. V., Jr. and J. F. Baytos. "The Differential Thermal Analysis Unit at Group GMX-3." Los Alamos Scientific Laboratory, University of California (1963). LAMS-2988.
10. Farmer, R. C. "The Velocity of Decomposition of High Explosives in a Vacuum." J. Chem Soc, 117, 1603 (1920).
11. "The Feasibility of Using Differential Thermal Analysis to Determine the Thermal Characteristics of Selected Primary Explosives." U. S. Naval Weapons Station (1961). NAVWEPS Report 6997. AD 262 573.
12. Finkelstein, R. J. and G. Gamov. "Theory of the Detonation Process." NAVORD Report 9046 (April 1947).
13. Johnson, O. H. "EMX as a Military Explosive." NAVORD Report 4371 (October 1956).
14. Kissinger, H. E. "Reaction Kinetics in Differential Thermal Analysis." Anal Chem, 29, 1702 (November 1957).

15. Kissinger, H. E. "Variation of Peak Temperature with Heating Rate in Differential Thermal Analysis." J. of Research of NBS, 57, 217 (October 1956).
16. Krein, G. "On Possibilities of Application of Differential Thermal Analysis.....in the Examination of Explosives." Explosivstoffe, 13, 205 (August 1956).
17. Leone, N. Private Communication, April 1967.
18. Macek, A. "Sensitivity of Explosives." Chemical Reviews, 62, 41 (1962).
19. Nelson, D. G. "Safety Techniques for Research and Development of New High Energy Oxidizers." J. Chem Ed, 43, A441 (May 1966).
20. O'Neill, M. J. "Measurement of Specific Heat Functions by Differential Scanning Calorimetry." Anal Chem, 38, 1331 (September 1966).
21. "Operational Safety Procedure for Building 101 Complex Chemical High Explosives Areas." Lawrence Radiation Laboratory, University of California, Livermore, California (April 1966).
22. Redfern, J. P. ed. Thermal Analysis 1965. Proceedings of the First International Conference on Thermal Analysis, Aberdeen, Scotland, September 1965. London: Macmillan, 1965.
23. Rideal, E. K. and A. J. B. Robertson. "The Sensitiveness of Solid High Explosives to Impact." Proc Roy Soc (London), A195, 135 (1948).
24. Robertson, A. J. B. J. Chem Ind (London), 61, 221 (1943).
25. Robertson, A. J. B. "The Thermal Decomposition of Explosives." Trans Faraday Soc, 45, 95 (1949).
26. Rogers, R. N. "The Simple Microscale Differential Thermal Analysis of Explosives." Microchemical Journal, 5, 91 (1961).
27. Rogers, R. N. and E. D. Morris, Jr. "Determination of Emissivities with a Differential Scanning Calorimeter." Anal Chem, 38, 410 (March 1966).
28. Rogers, R. N. and E. D. Morris, Jr. "On Estimating Activation Energies with a Differential Scanning Calorimeter." Anal Chem, 38, 412 (March 1966).
29. Rojinski, S. Z. Physik Chem, B18, 364 (1932).
30. Sax, N. I. Dangerous Properties of Industrial Materials. New York: Reinhold, 1957.

31. Scullion, E. J. "A Survey of the Methods Available for the Analysis of HMX/RDX Mixtures." Chemical Inspectorate, Royal Arsenal, London (April 1965). AD 479 417.
32. Smothers, W. J., and Y. Chiang. Handbook of Differential Thermal Analysis. New York: Chemical Publishing, 1966.
33. Stein, F. P. "Time to Explosion for an Explosive Subjected Externally to Elevated Temperatures." Picatinny Arsenal Technical Report 3167, March 1965. AD 459 649.
34. Thermal Analysis Newsletter, Number 4, Perkin-Elmer Corporation, Norwalk, Connecticut.
35. Thermal Analysis Newsletter, Number 5, Perkin-Elmer Corporation, Norwalk, Connecticut.
36. Thermal Analysis Newsletter, Number 6, Perkin-Elmer Corporation, Norwalk, Connecticut.
37. Timmerman, J. Physico-Chemical Constants of Binary Systems in Concentrated Solutions. Vols I, II. New York: Interscience Publishers, 1959.
38. Tomlinson, W. R. "Properties of Explosives of Military Interest." Picatinny Arsenal Technical Report 1740, 1963. AD 457 747.
39. Van Geel, J. L. C. "Safe Radius of Heat Generating Substances." Ind and Eng Chem, 58, 24 (January 1966).

Appendix A

Signature Thermograms

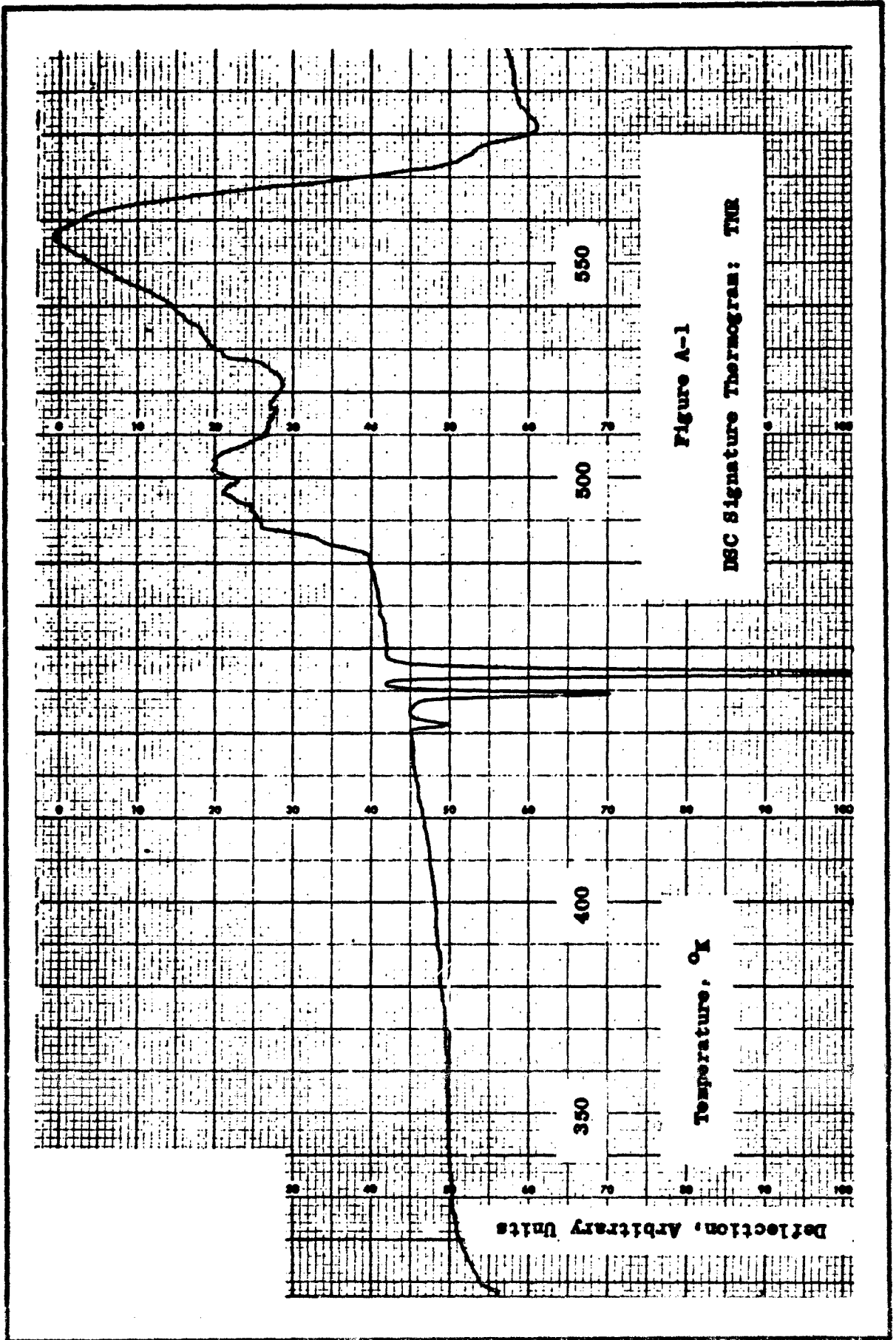


Figure A-1
DSC Signature Thermogram: TNR

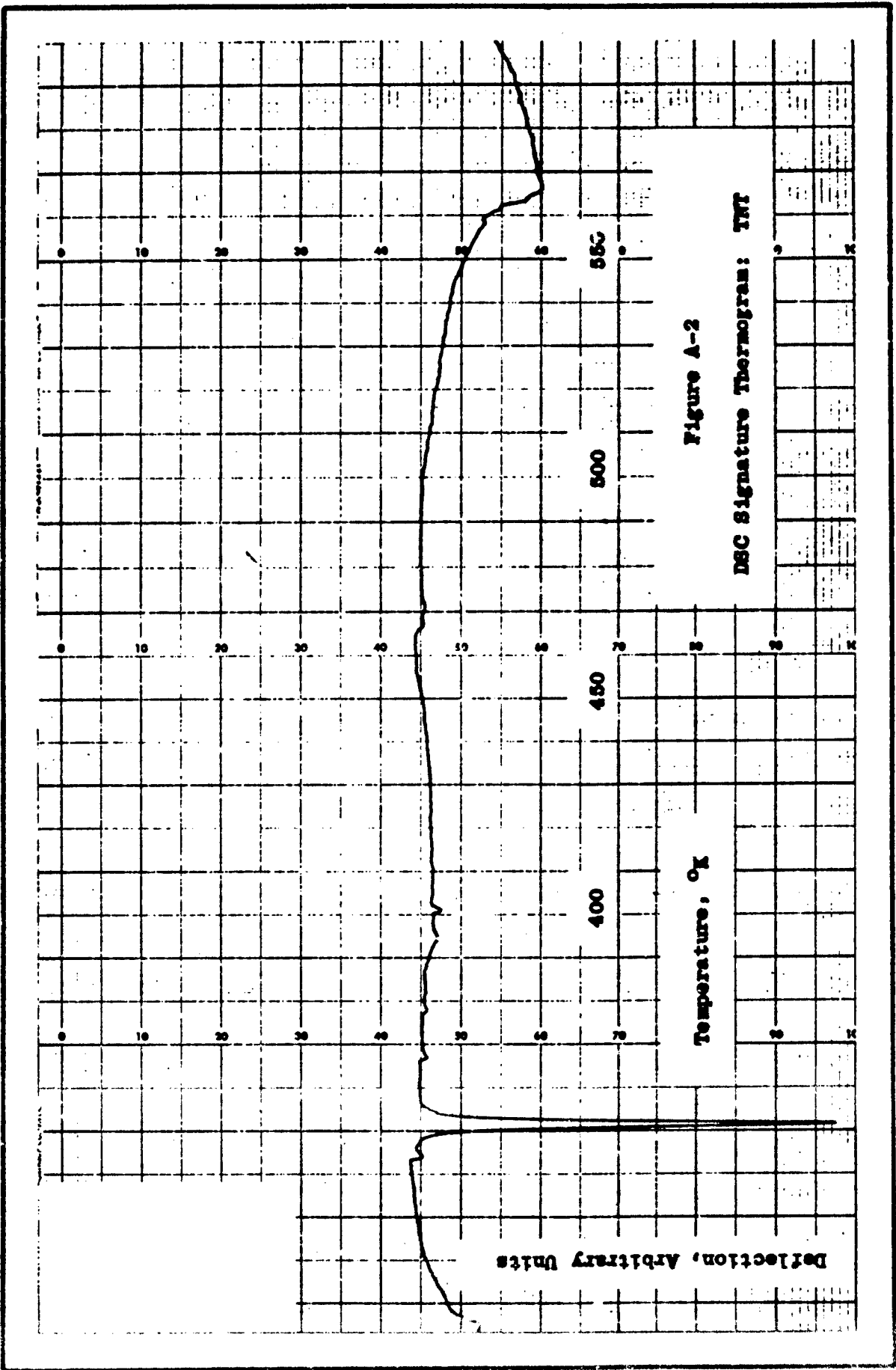


Figure A-2
DSC Signature Thermogram: TNT

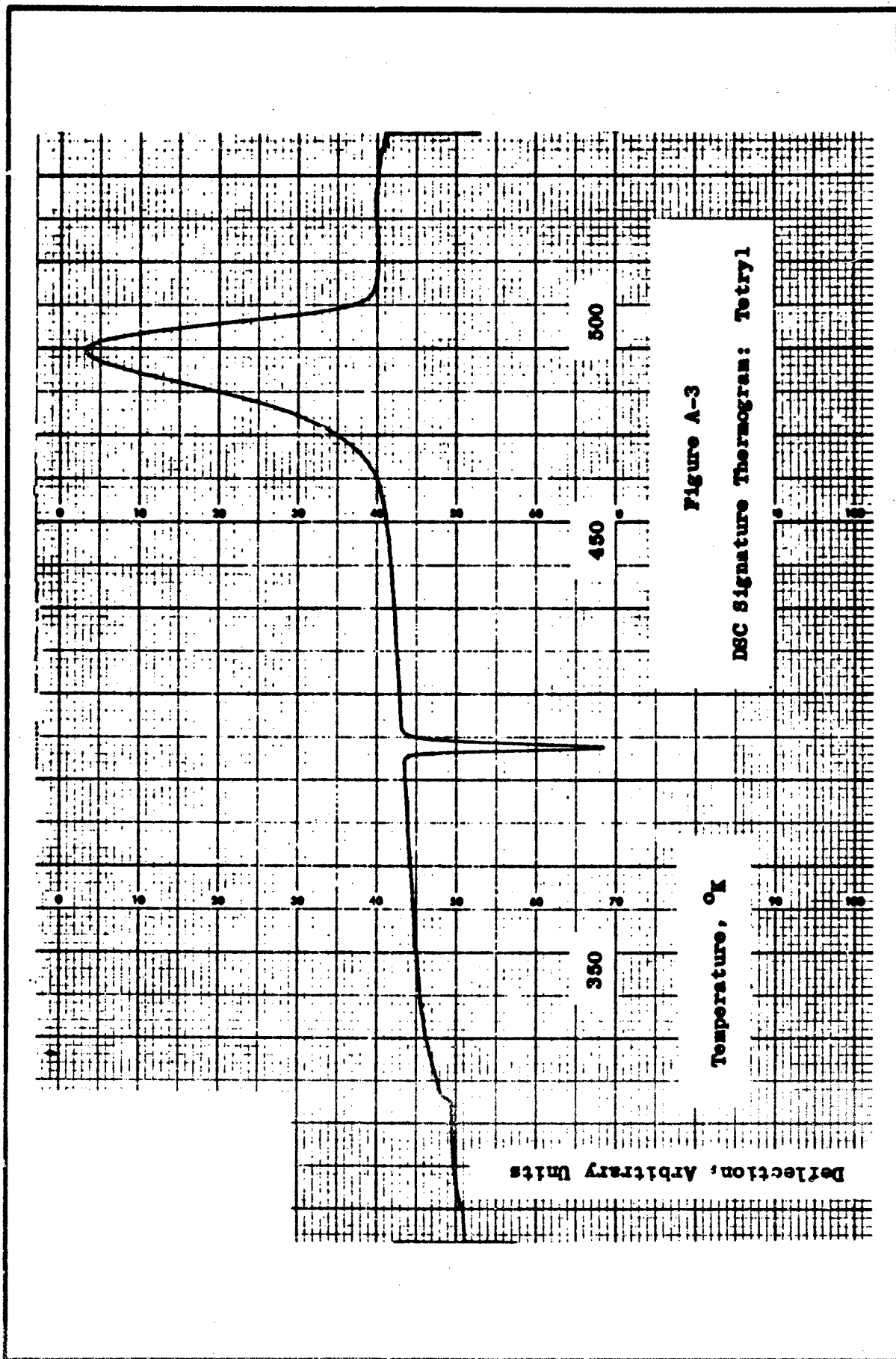


Figure A-3
DSC Signature Thermogram: Tetryl

Deflection, Arbitrary Units

Temperature, °C

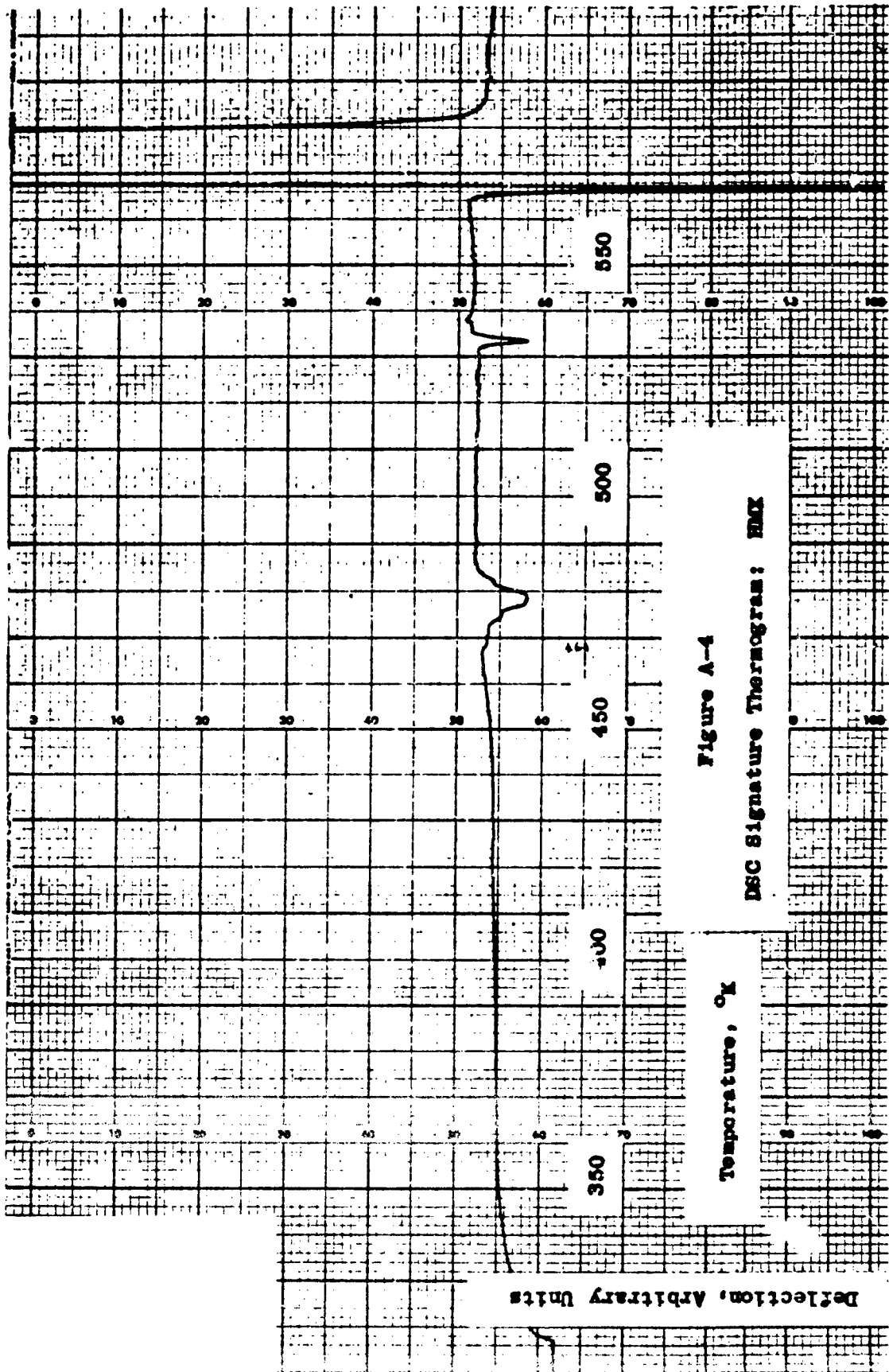


Figure A-4
DSC Signature Thermogram: HMX

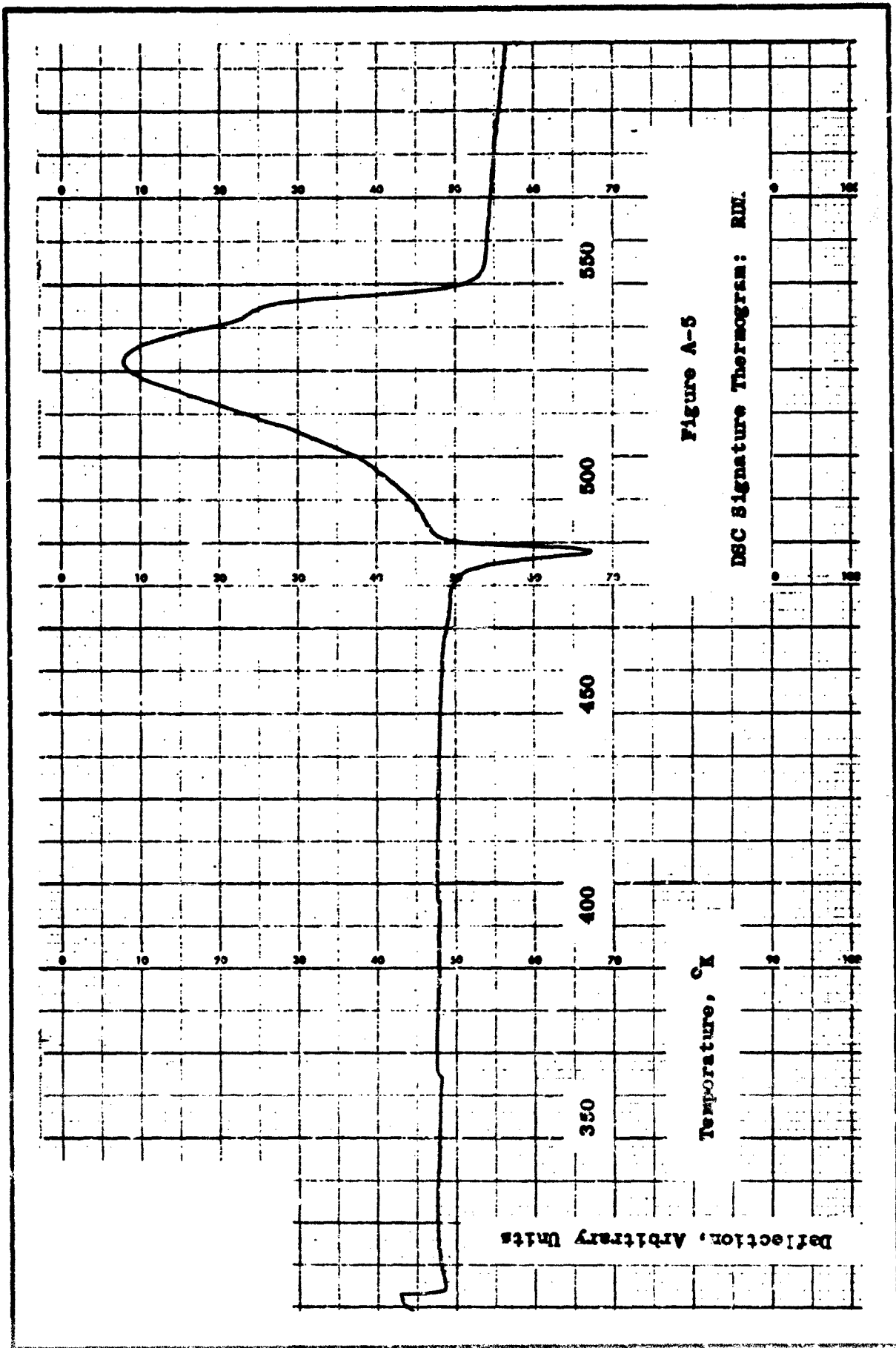
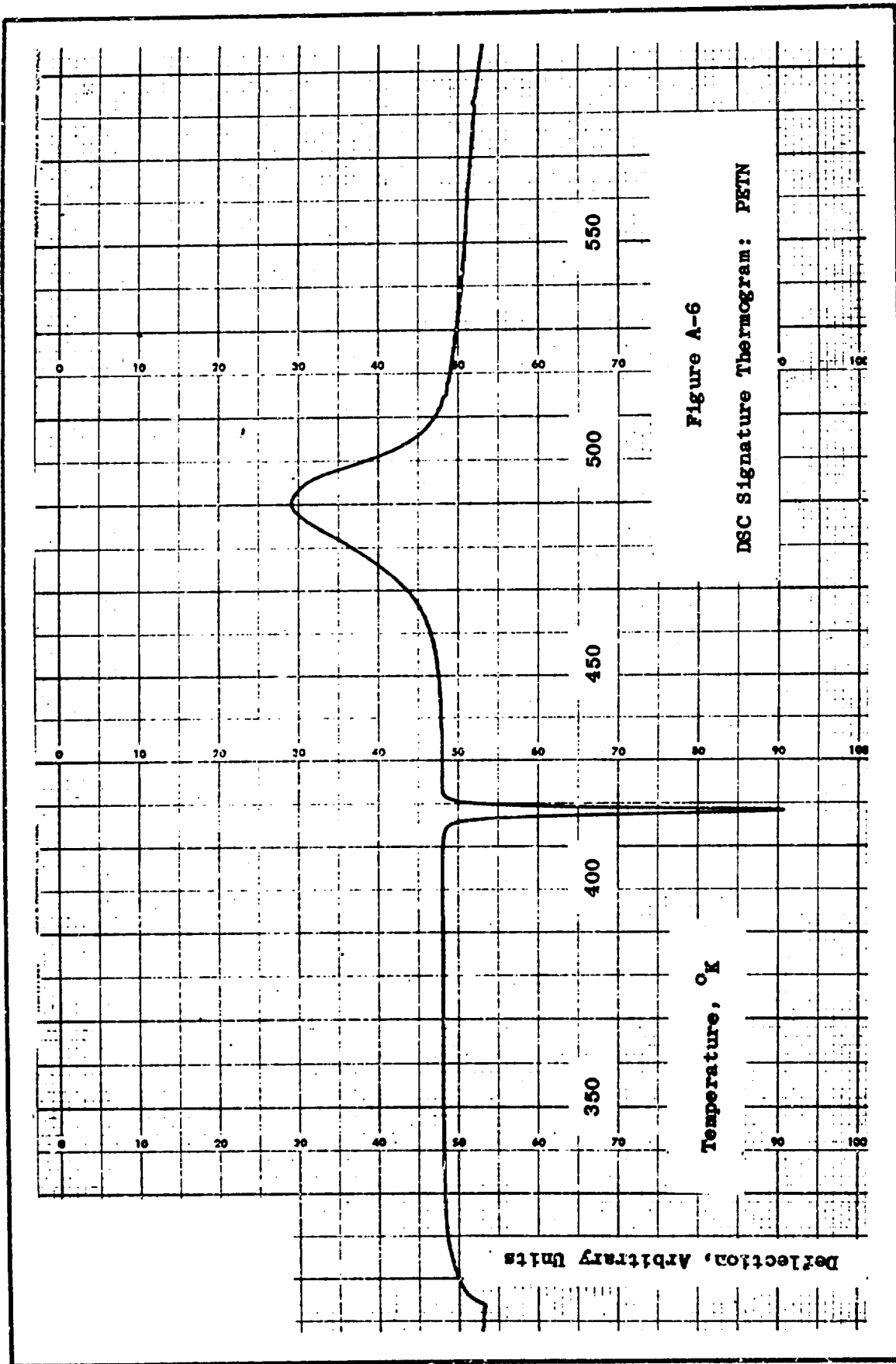


Figure A-5
DSC Signature Thermogram: R11.



Appendix B

Purity Endotherms, Calculations, and Data Plots

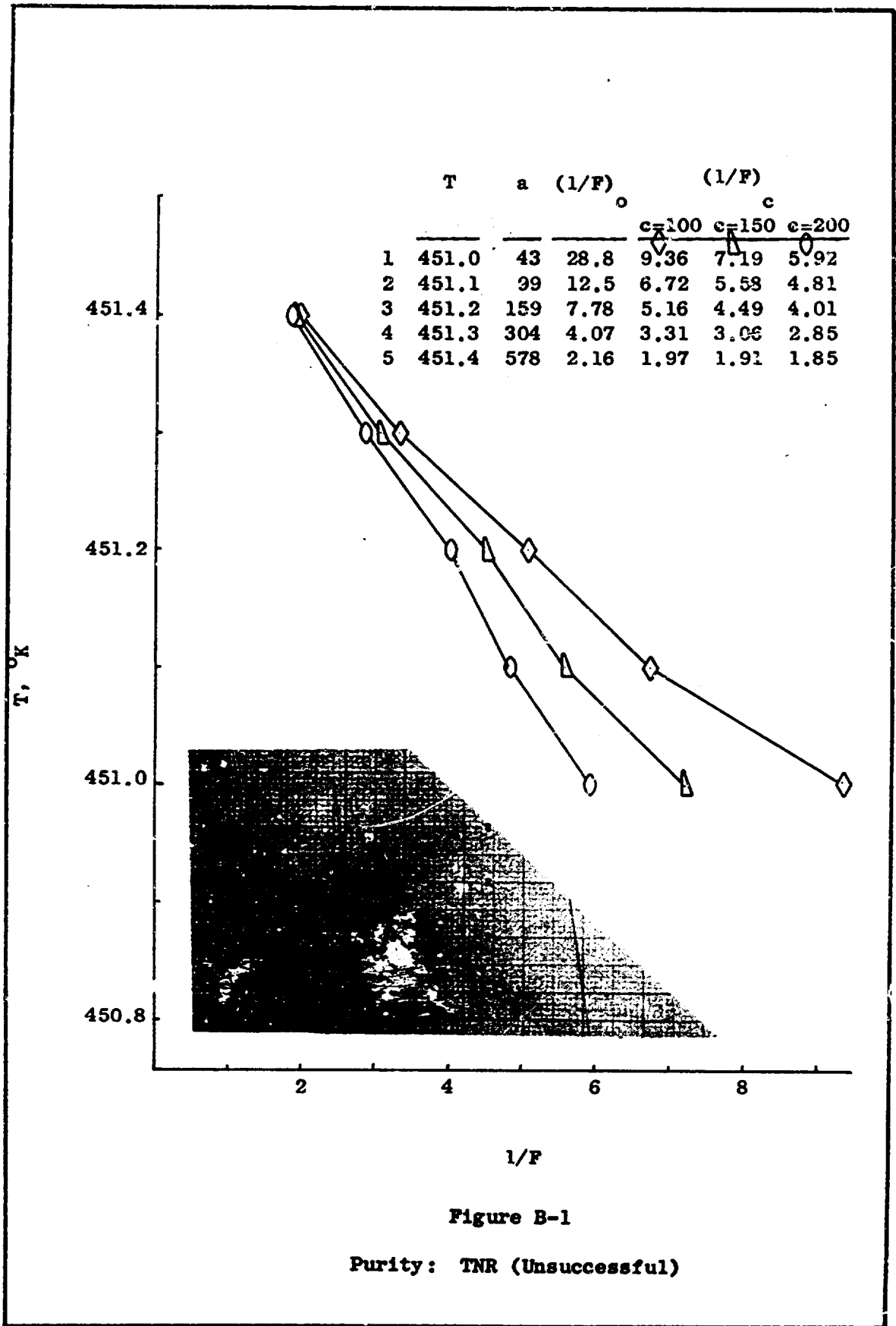


Figure B-1

Purity: TNR (Unsuccessful)

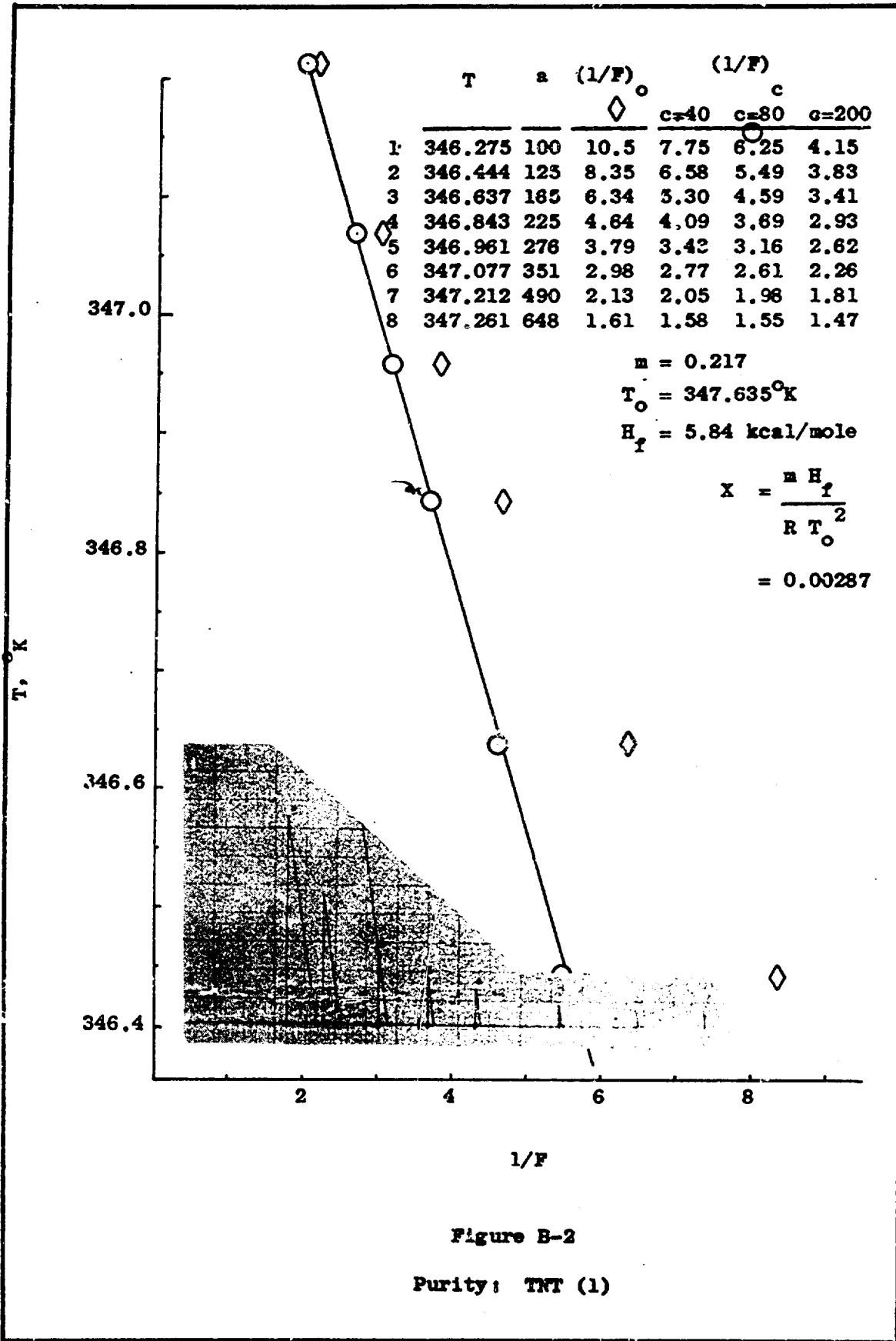


Figure B-2

Purity: TNT (1)

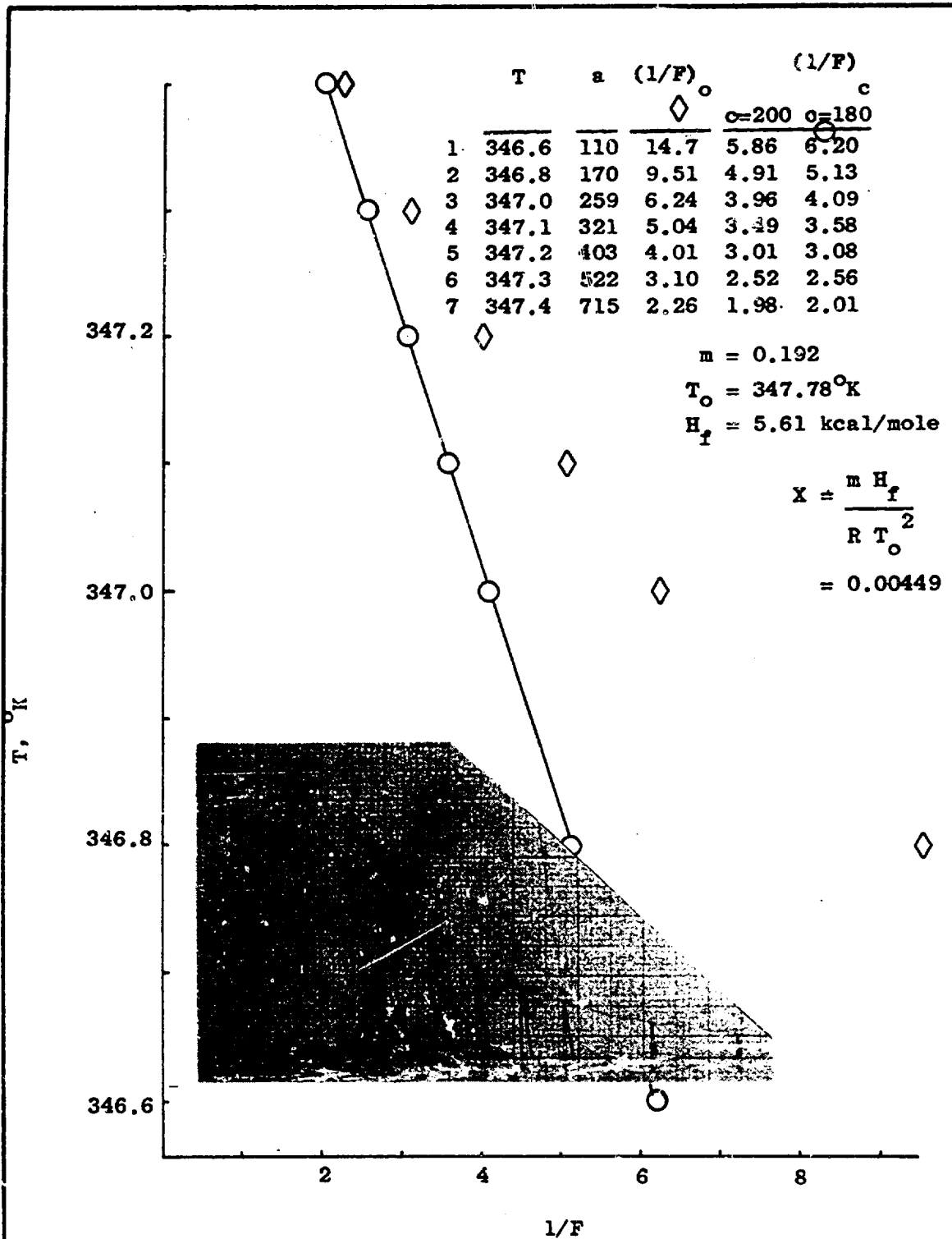


Figure B-3
Purity: TNT (2)

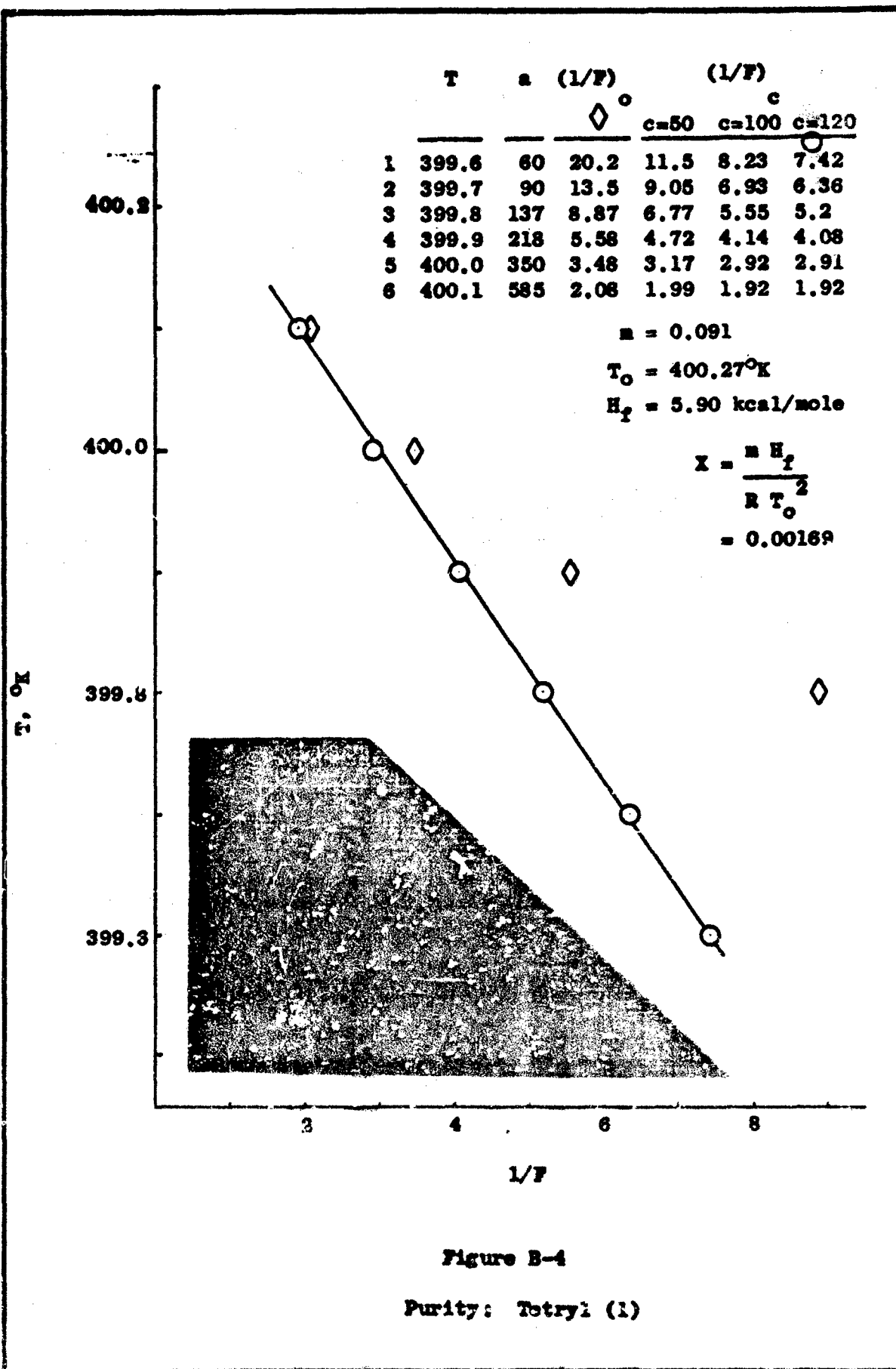


Figure B-4

Purity: Totryl (1)

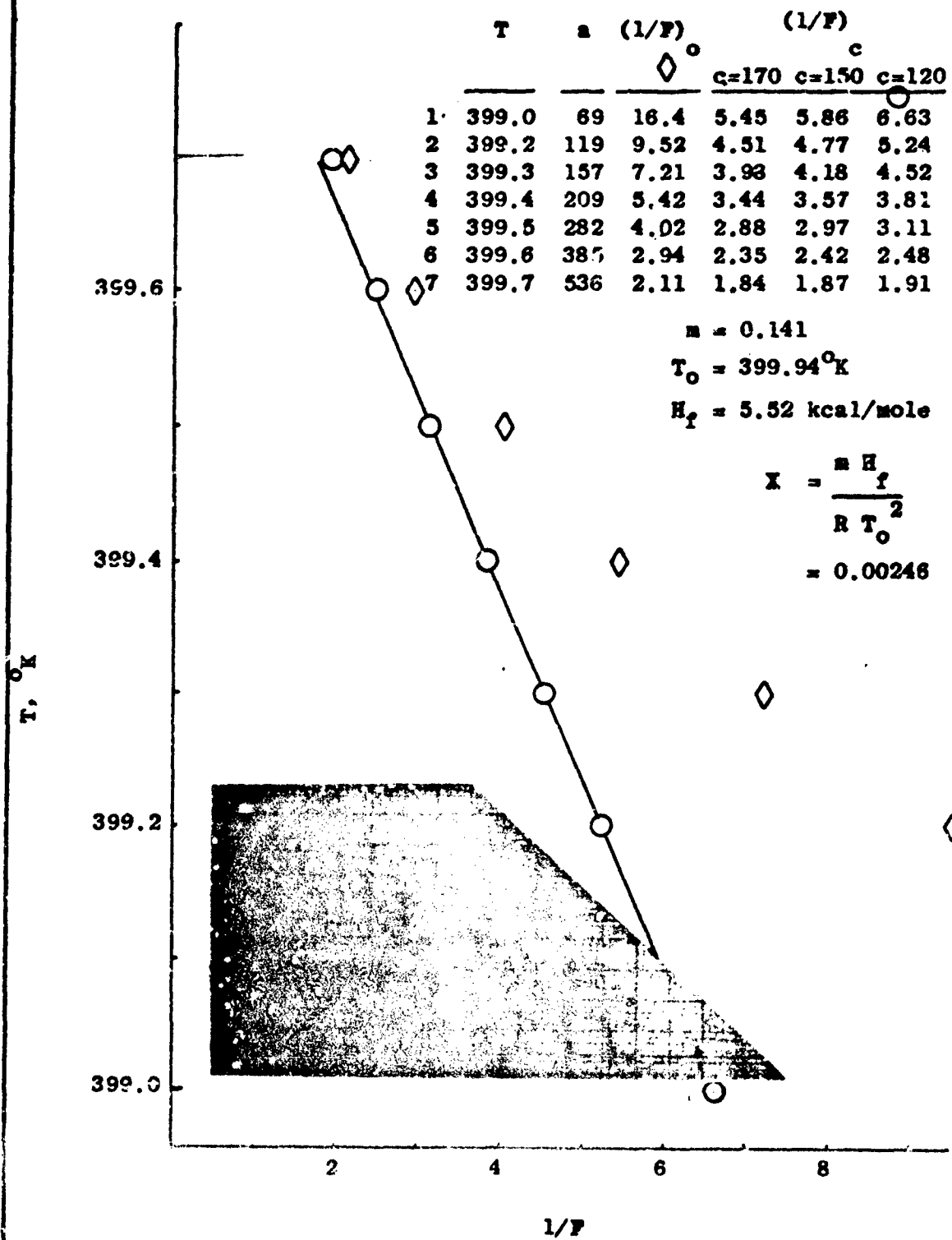


Figure B-5

Purity: Tetryl (2)

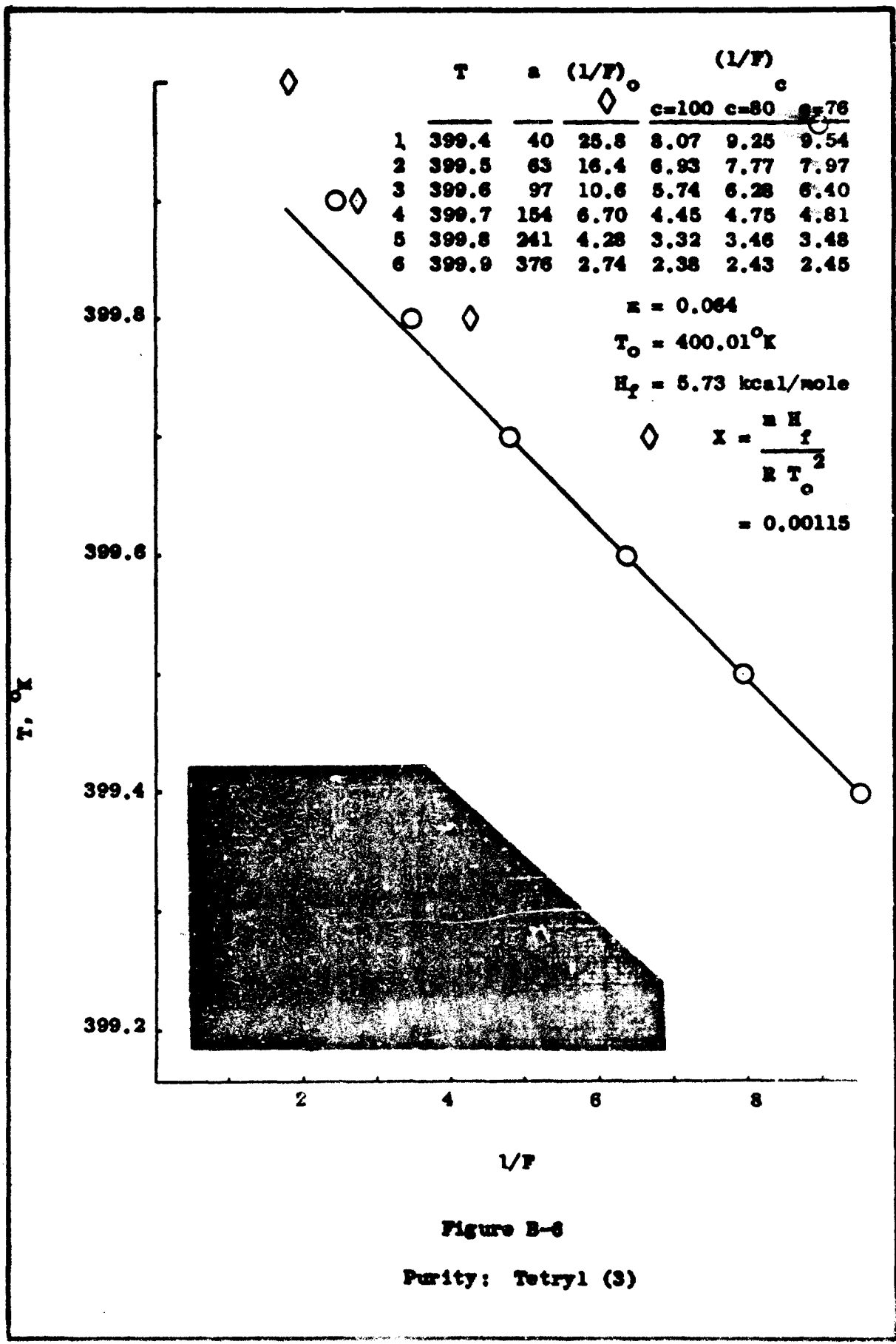


Figure B-6
Purity: Tetryl (3)

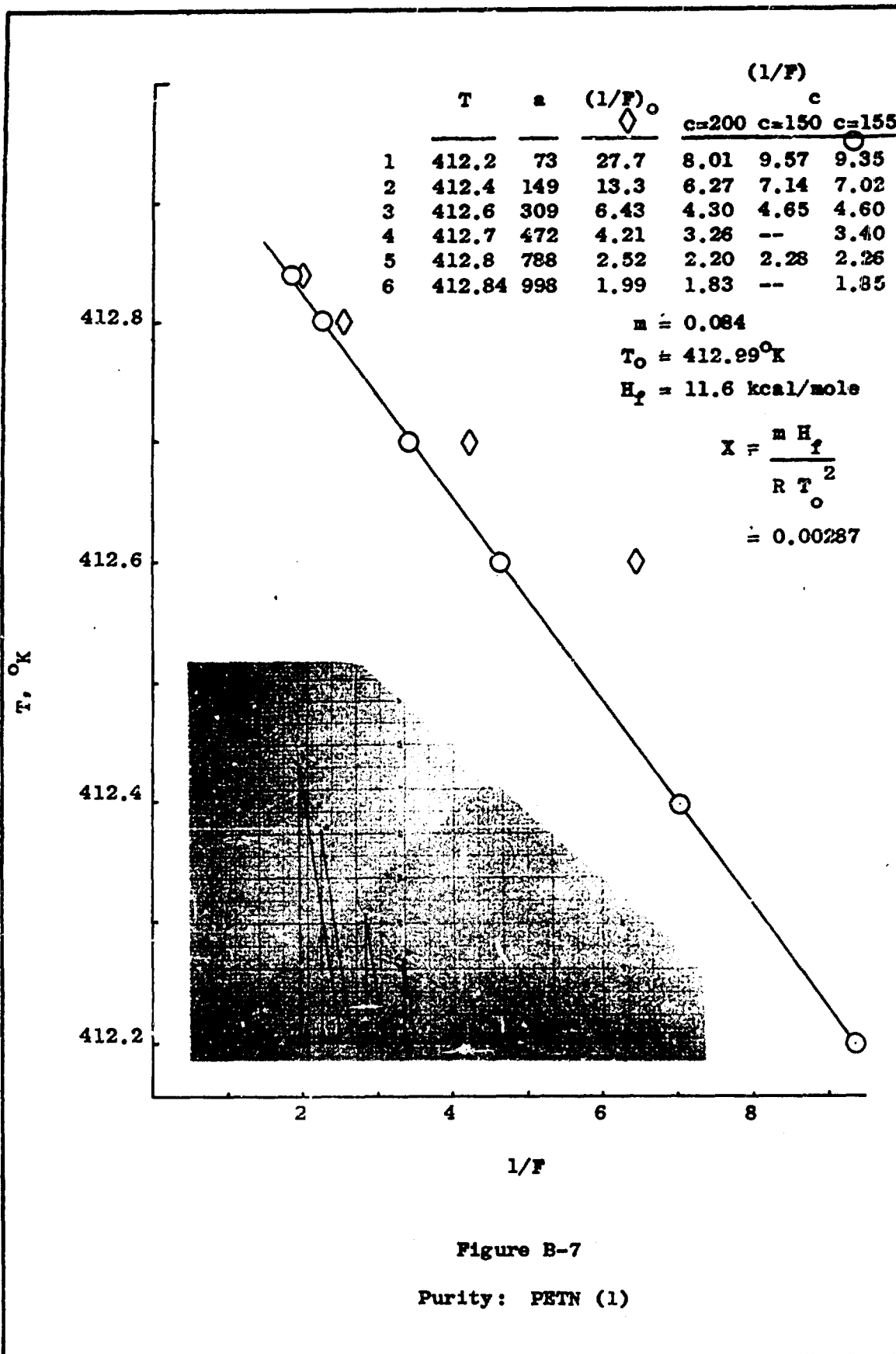
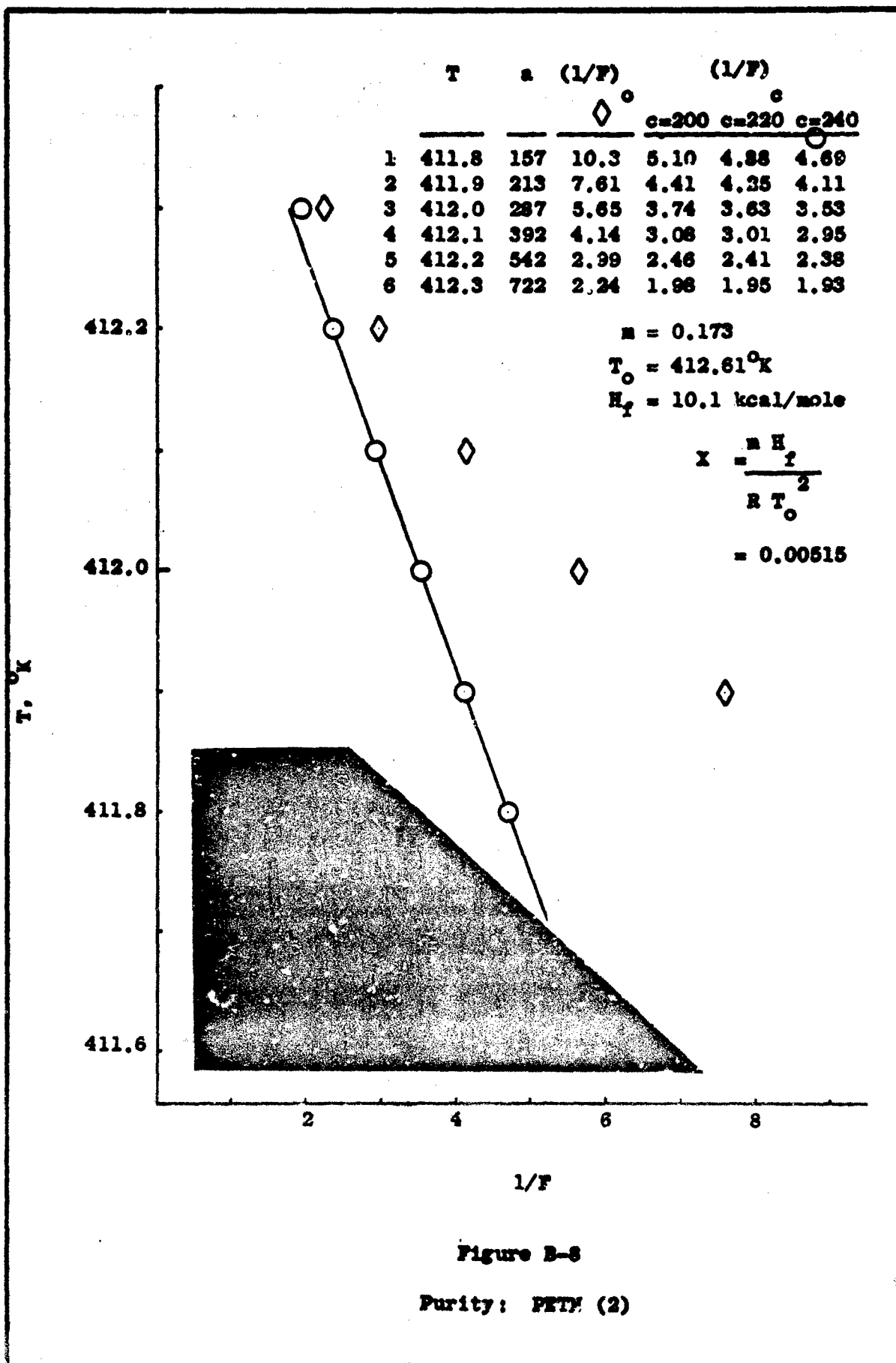


Figure B-7

Purity: PETN (1)



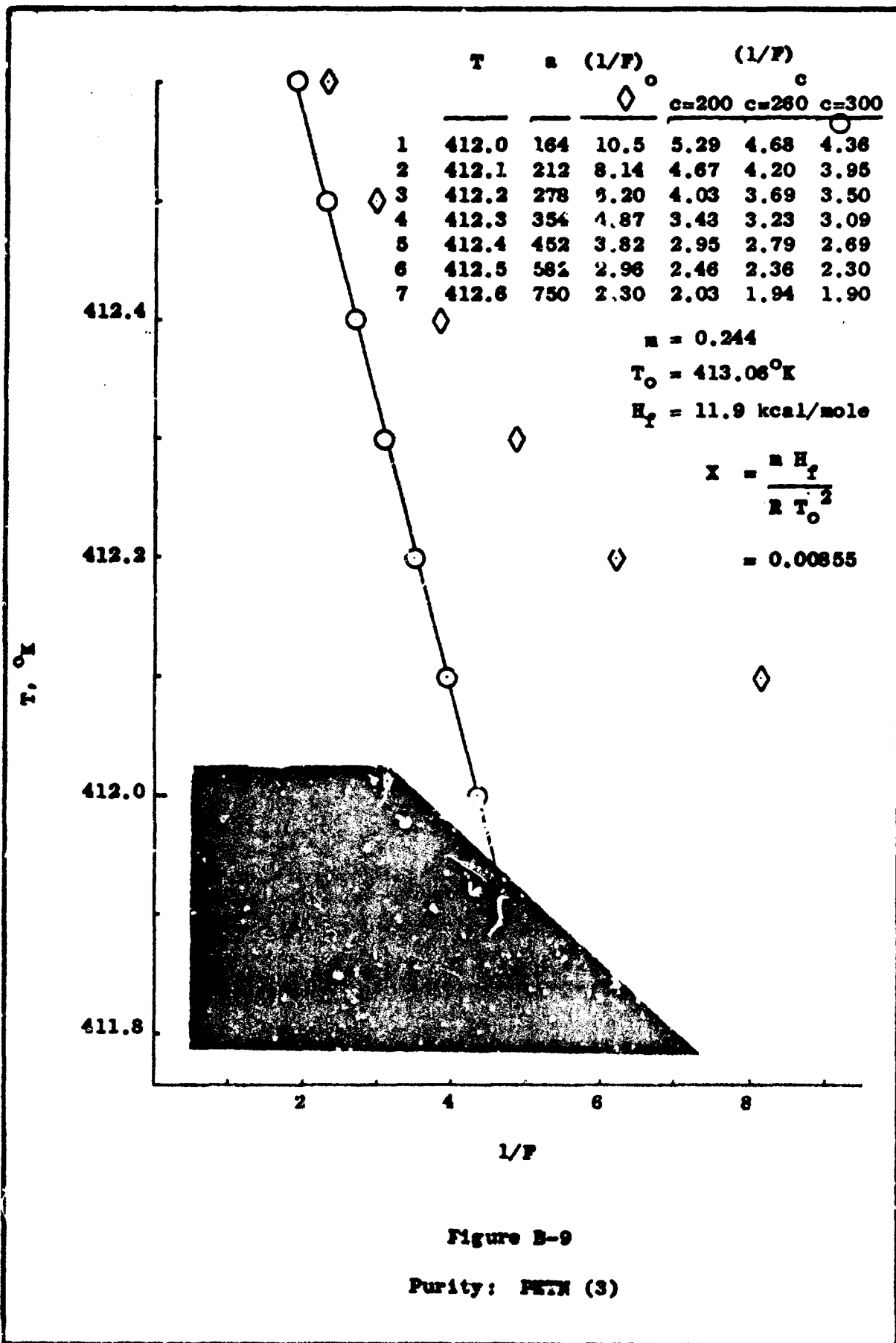
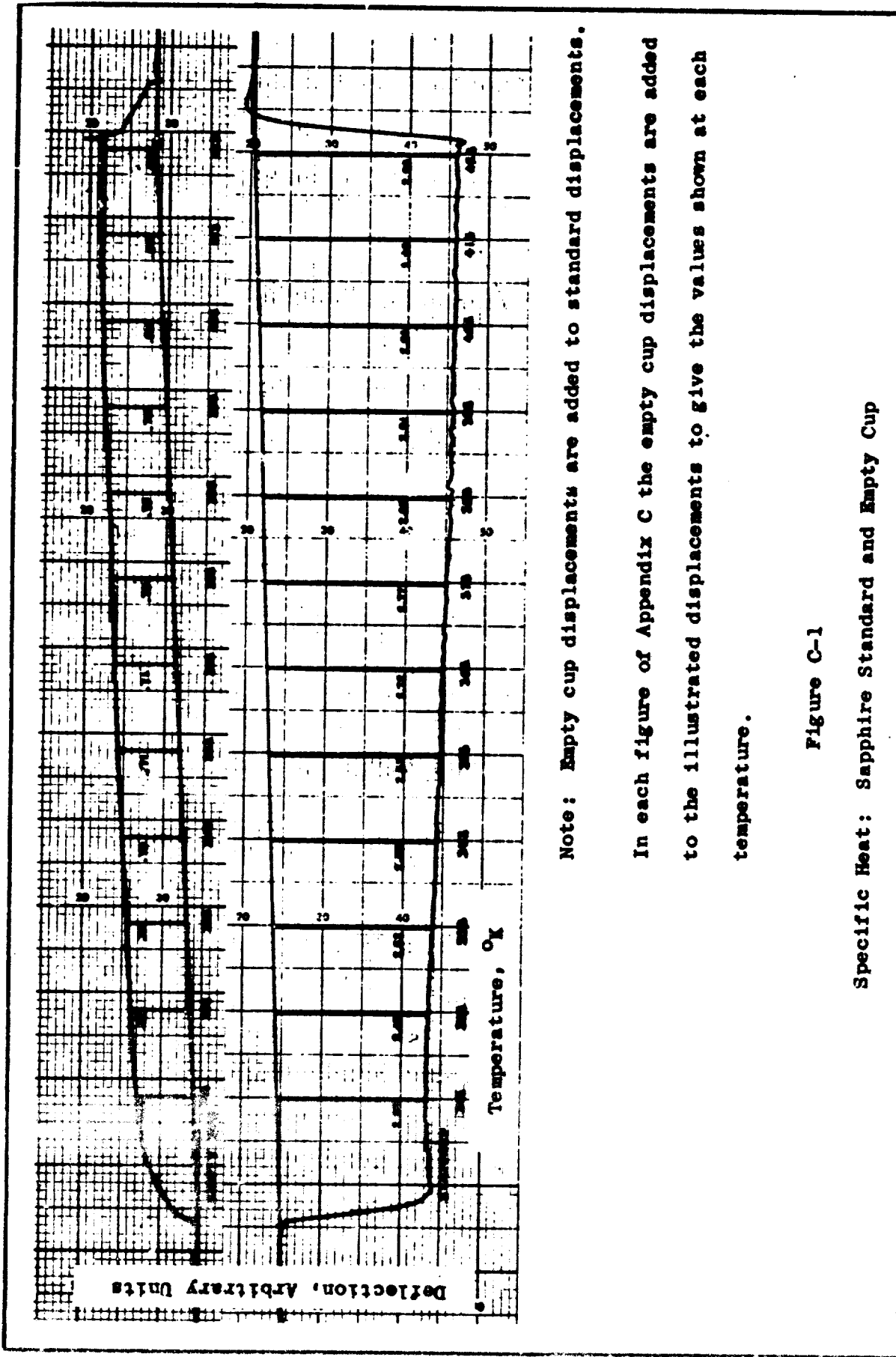


Figure B-9

Purity: PETM (3)

Appendix C

Specific Beat Traces and Comparative Data Plots



Note: Empty cup displacements are added to standard displacements.

In each figure of Appendix C the empty cup displacements are added to the illustrated displacements to give the values shown at each temperature.

Figure C-1

Specific Heat: Sapphire Standard and Empty Cup

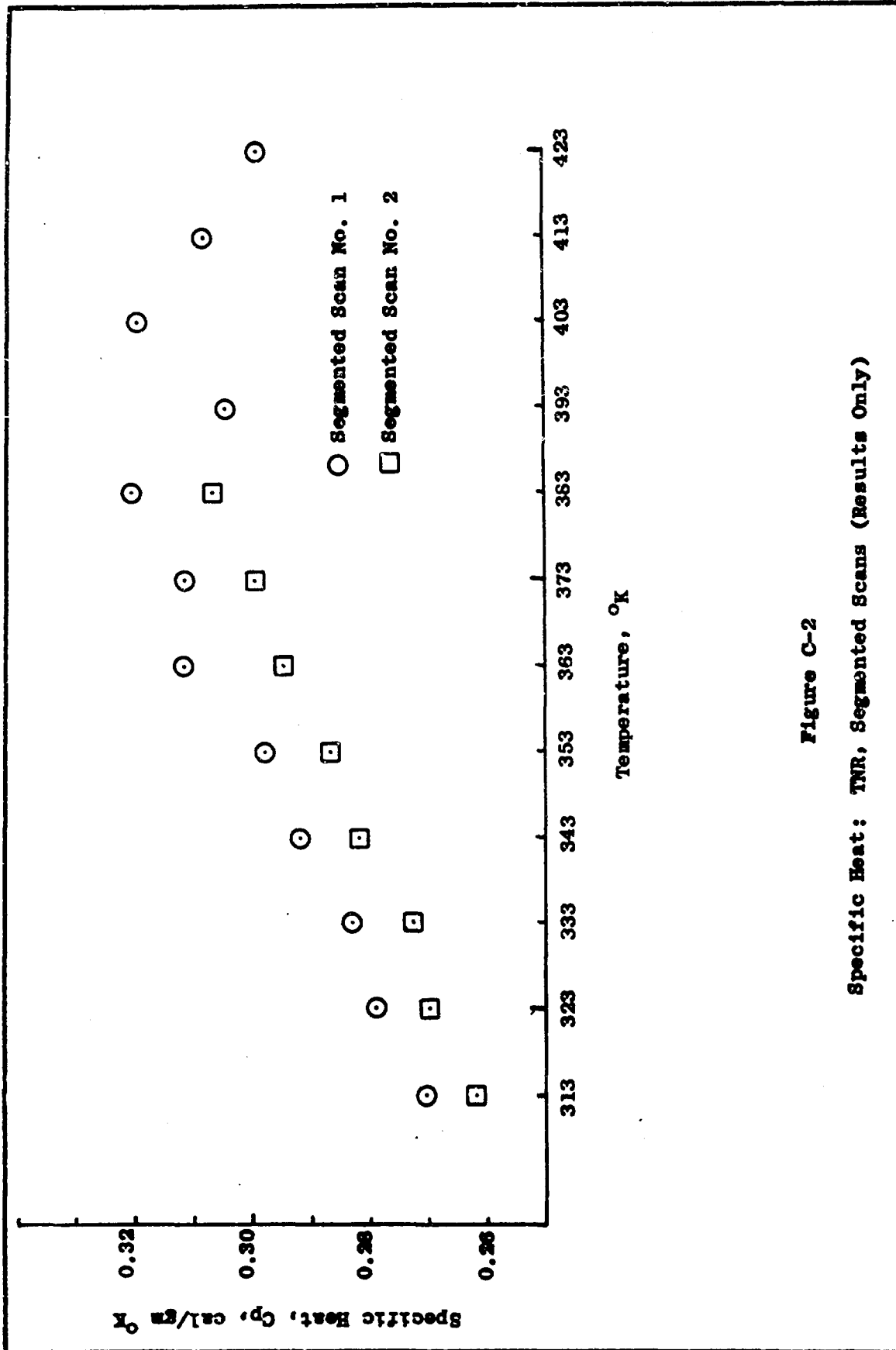


Figure C-2
Specific Heat: TNR, Segmented Scans (Results Only)

Specific Heat, C_p , cal/gm $^{\circ}K$

Δ \square
 \triangle \circ
 \square \circ
 \triangle \square \circ

\circ Segmented Scan No. 1
 \square Segmented Scan No. 2
 \triangle Continuous Scan

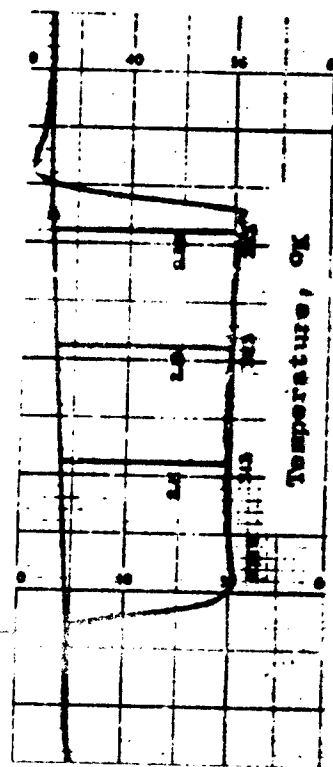


Figure C-3

Specific Heat: TWT, Continuous and Segmented Scans

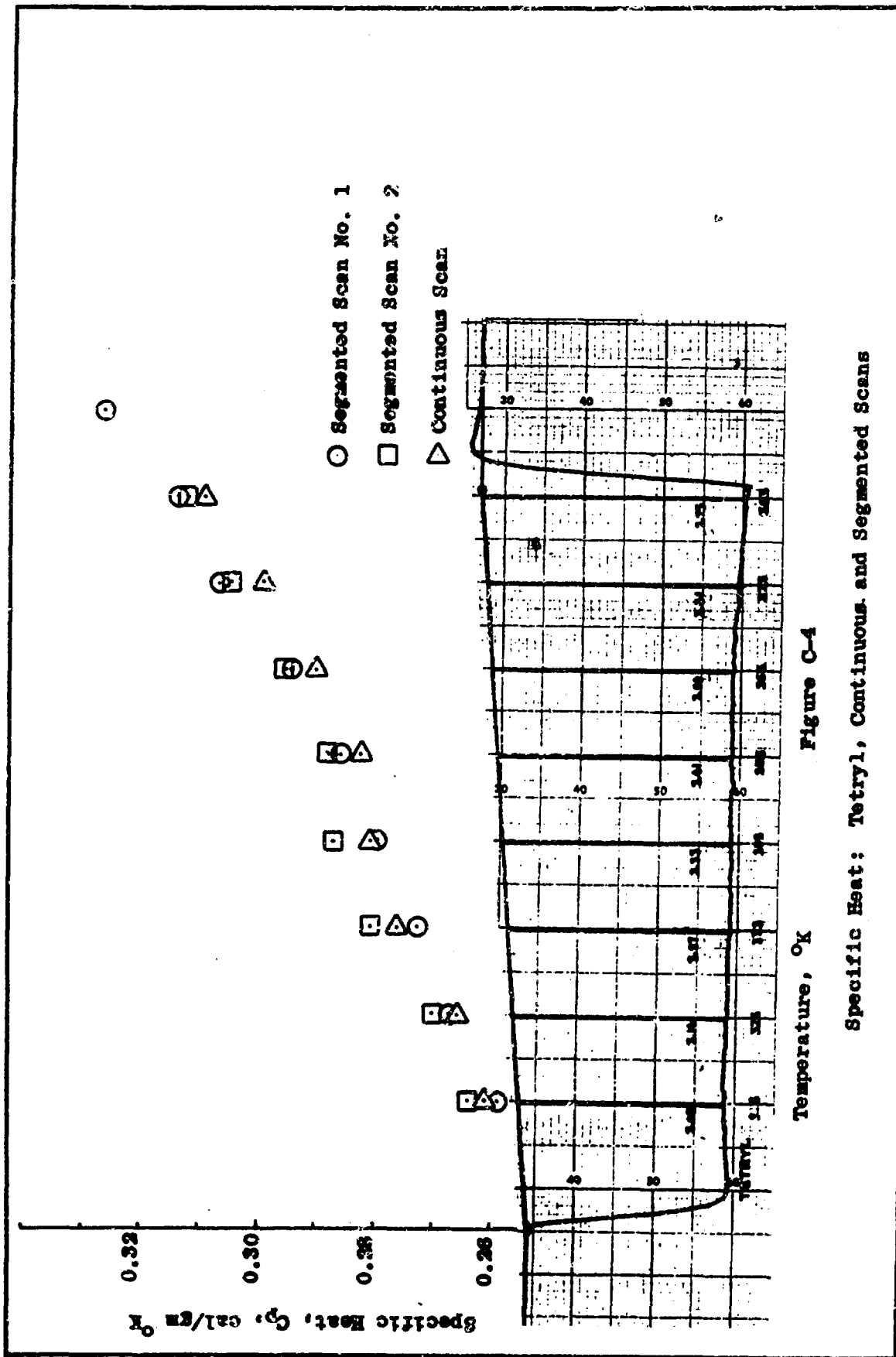


Figure C-4

Specific Heat: Tetryl, Continuous and Segmented Scans

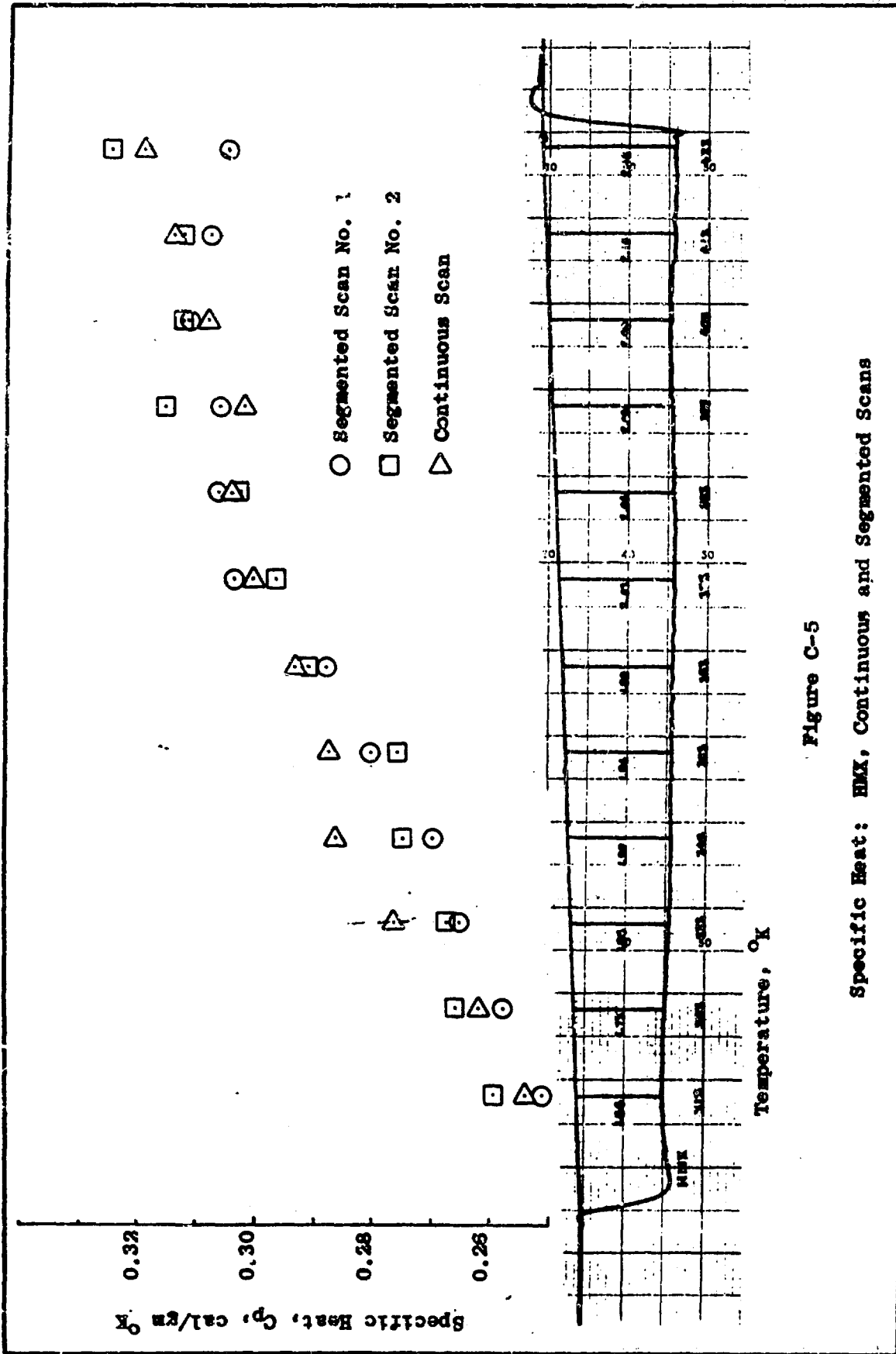


Figure C-5

Specific Heat: HMX, Continuous and Segmented Scans

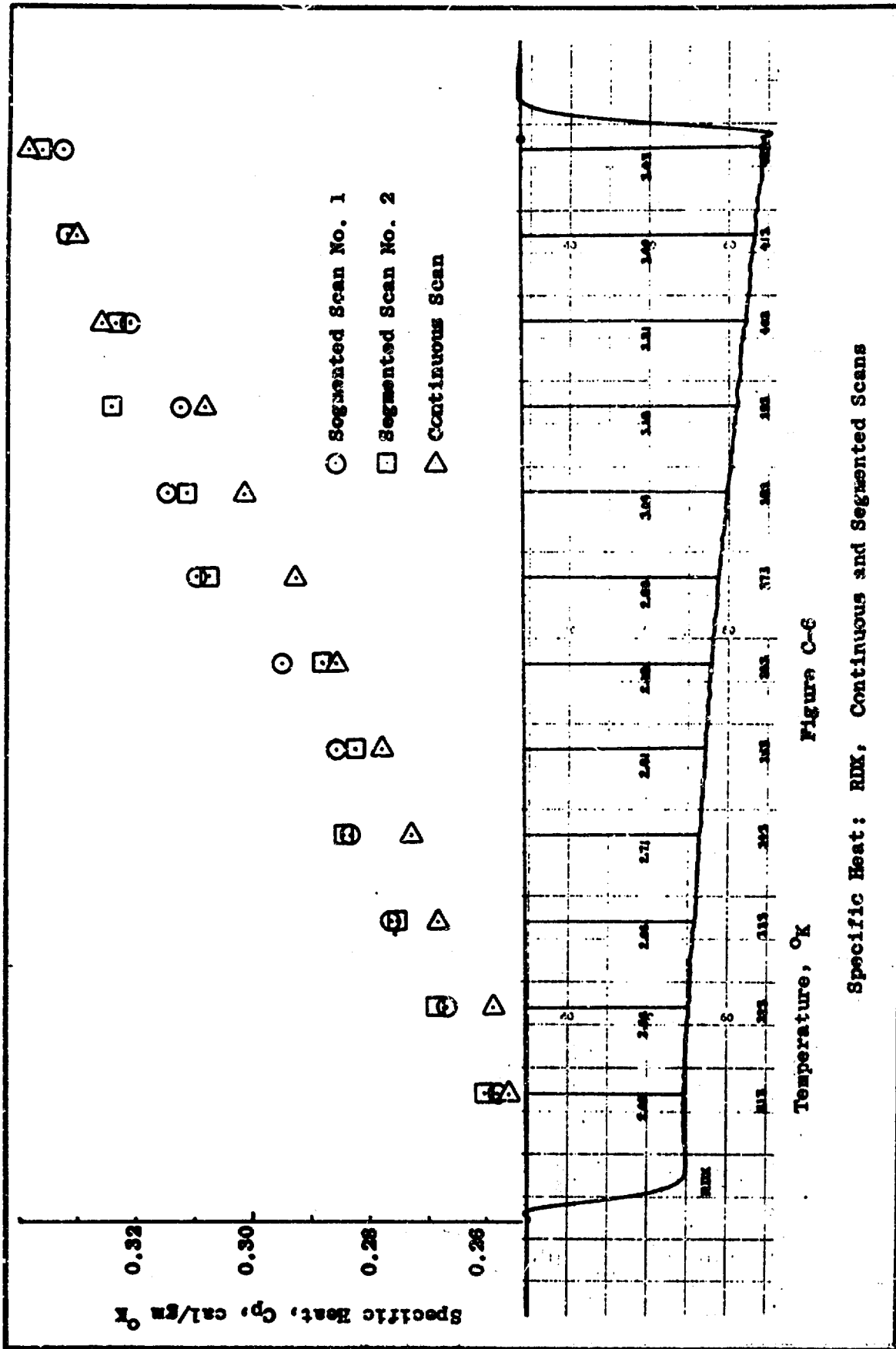


Figure C-6
Specific Heat: RDX, Continuous and Segmented Scans

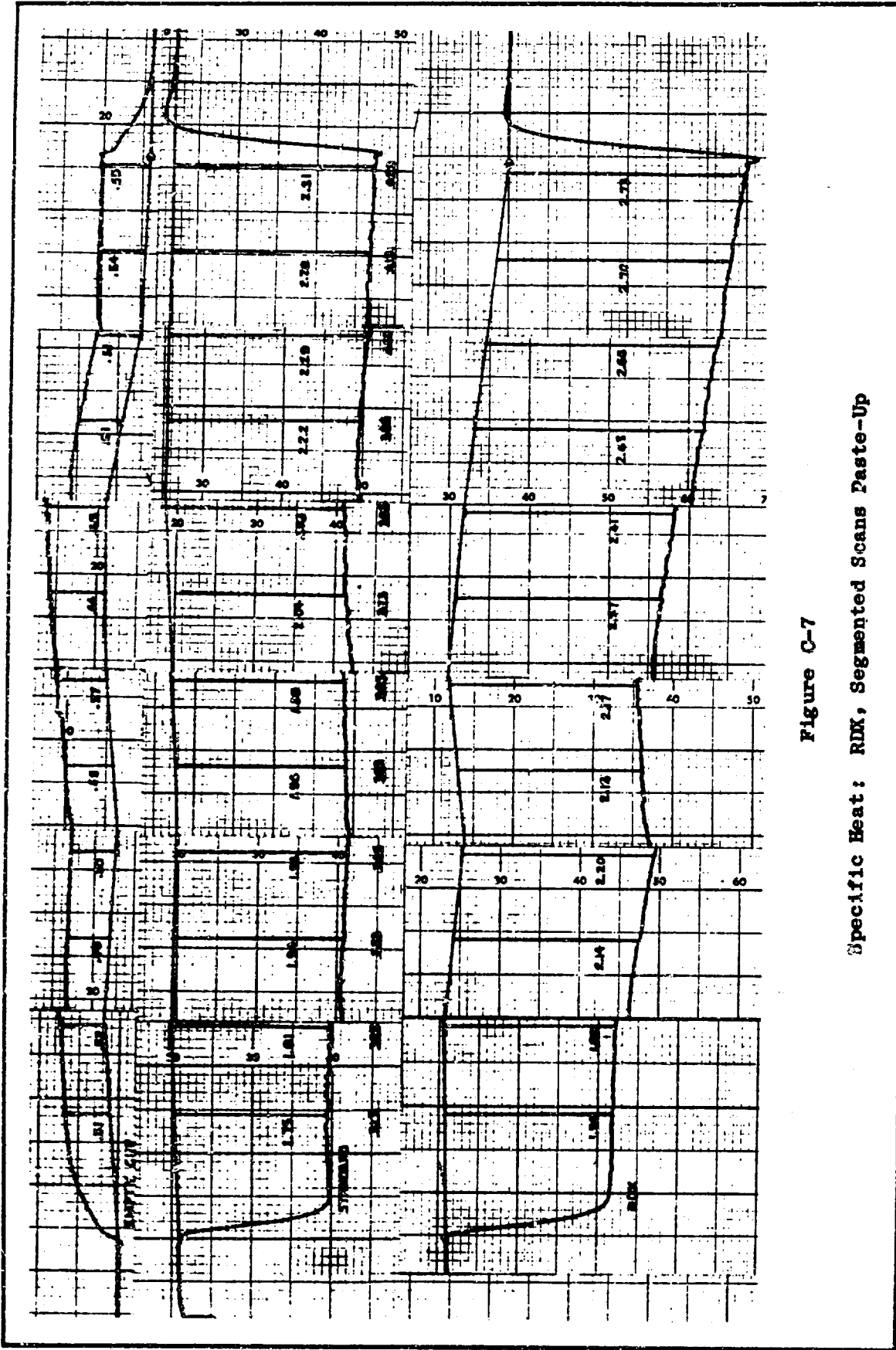
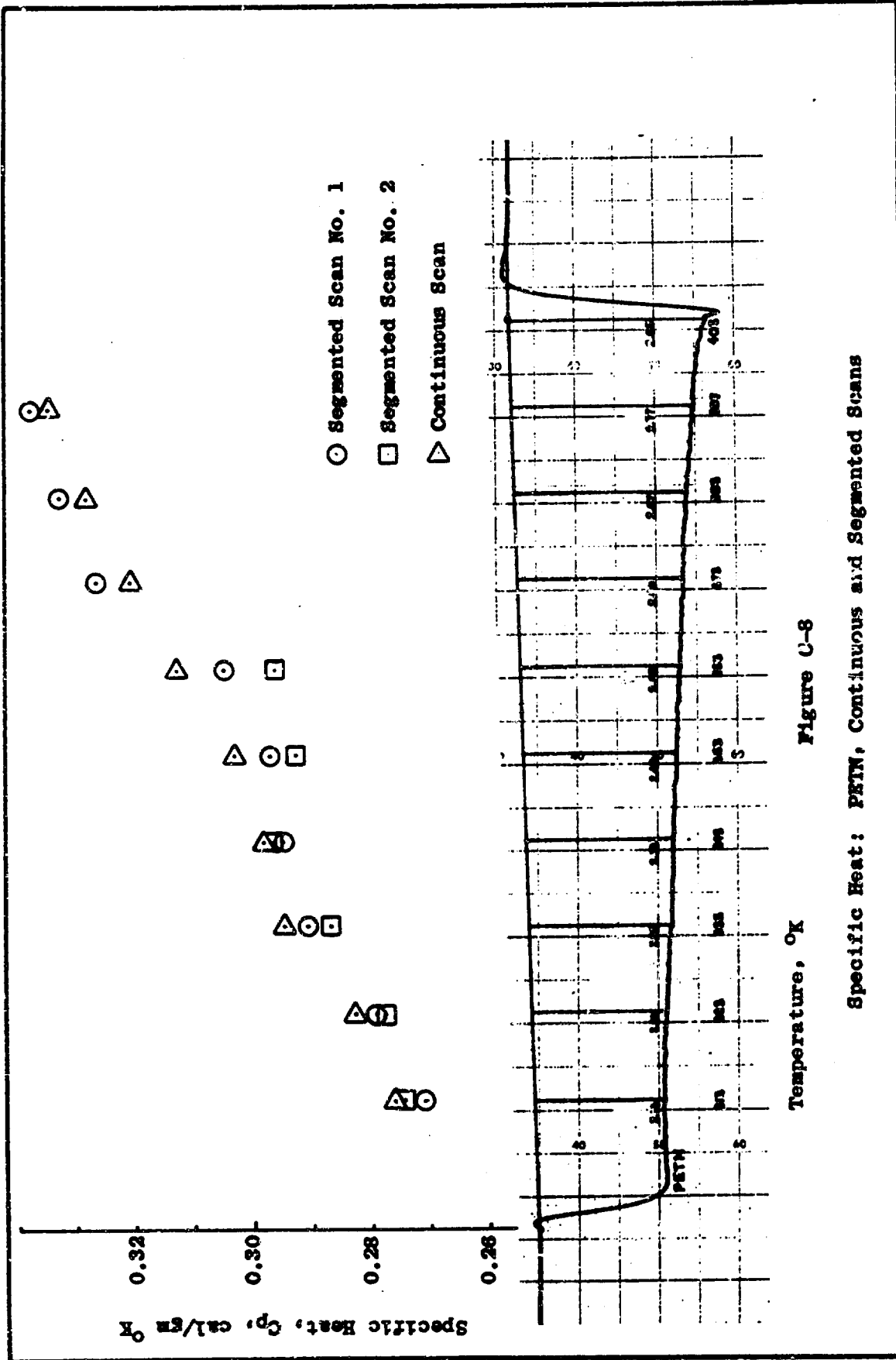


Figure C-7

Specific Heat: RDX, Segmented Scans Paste-Up



Appendix D

Activation Energy Exotherms, Calculations, and Data Plots

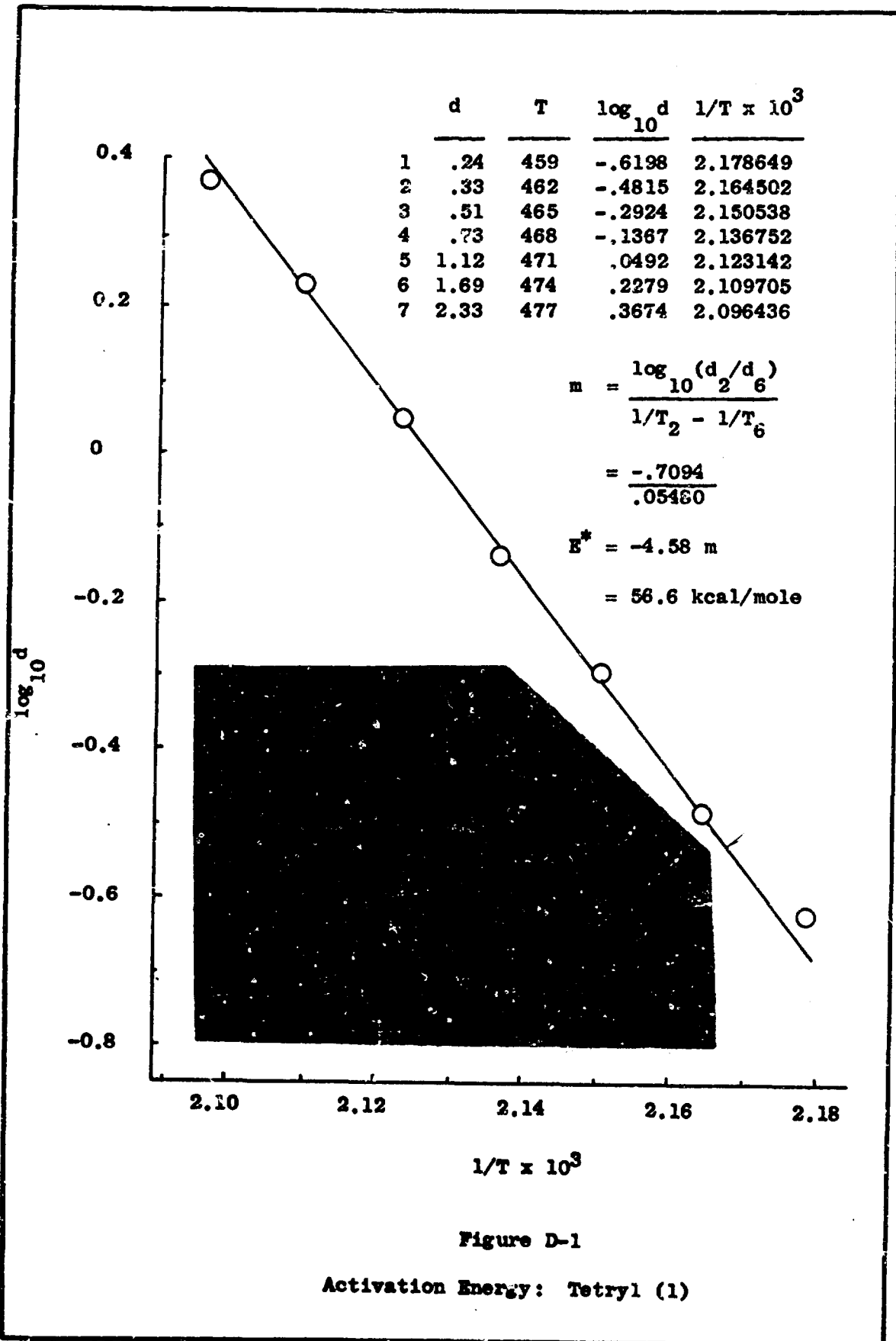


Figure D-1

Activation Energy: Tetryl (1)

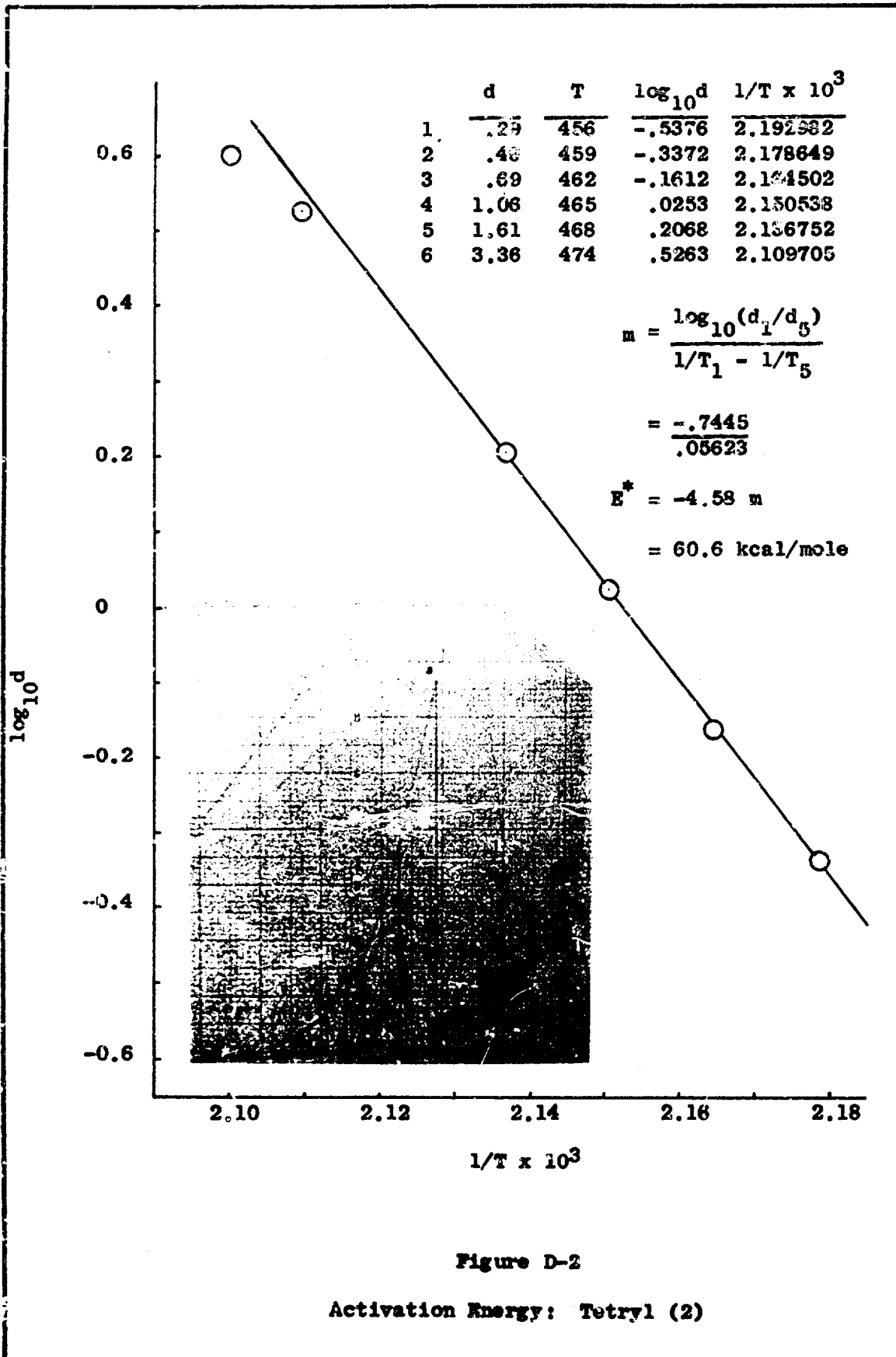


Figure D-2

Activation Energy: Tetryl (2)

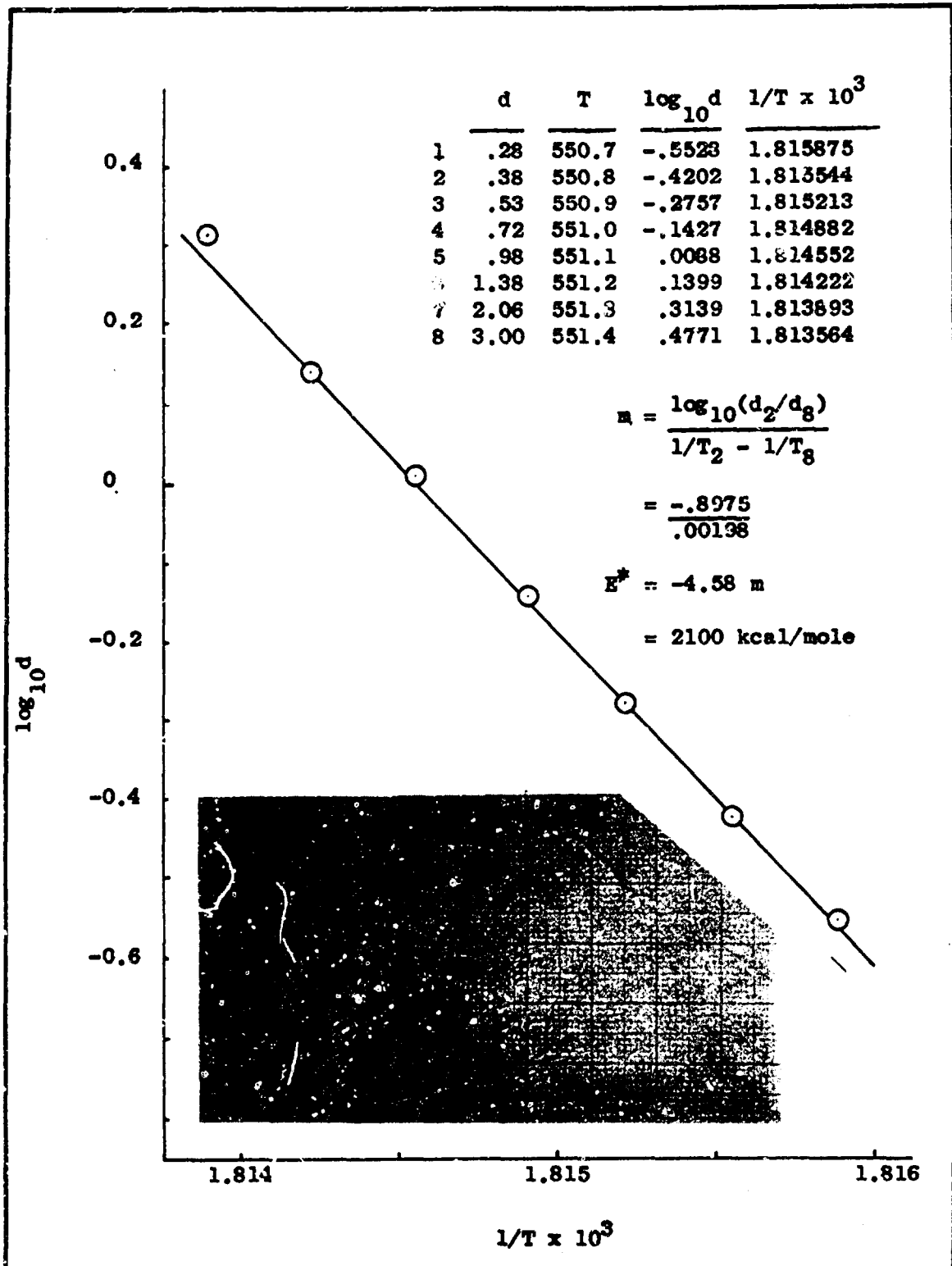


Figure D-3

Activation Energy: HMX (1)

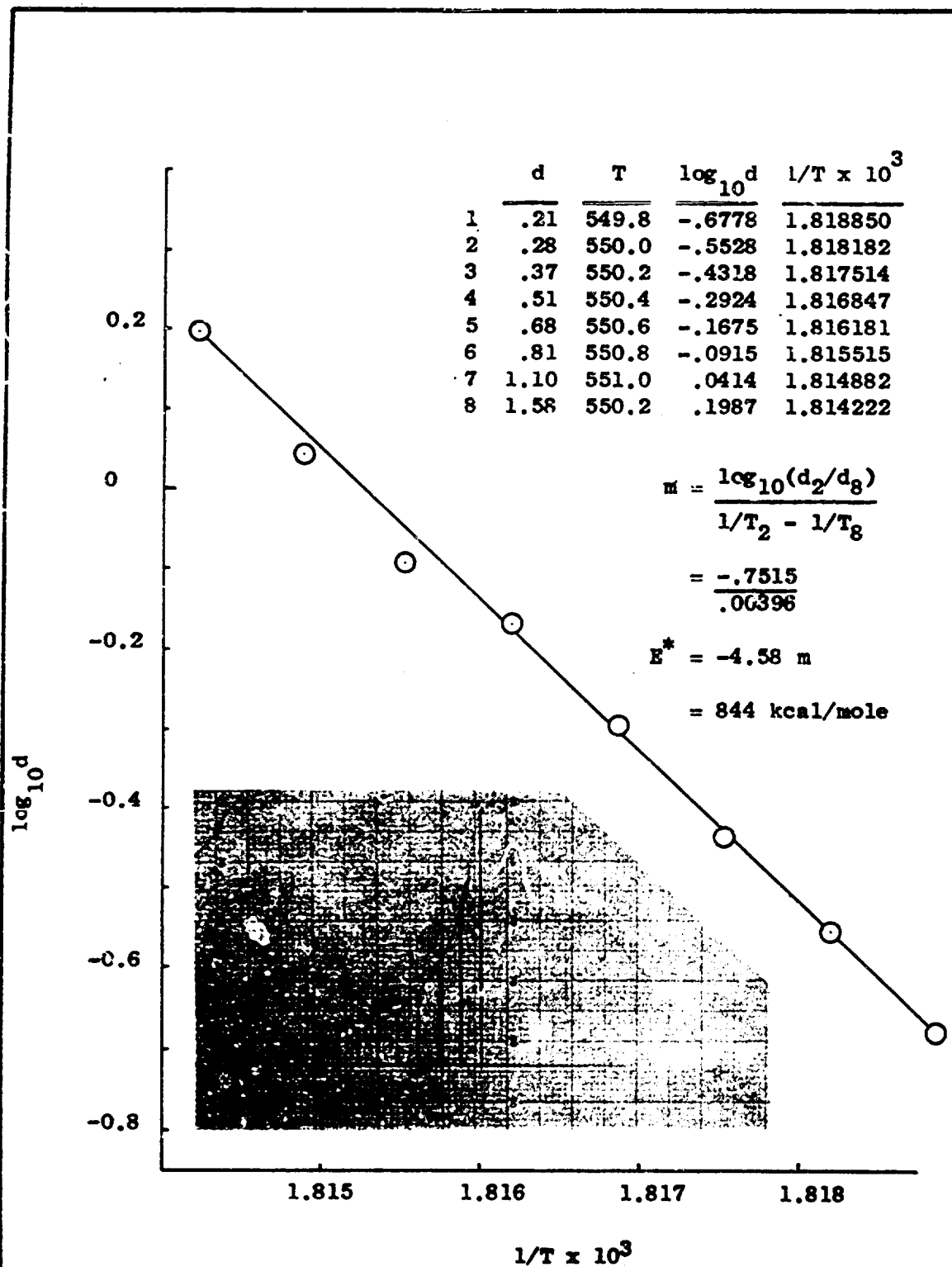


Figure D-4

Activation Energy: HMK (2)

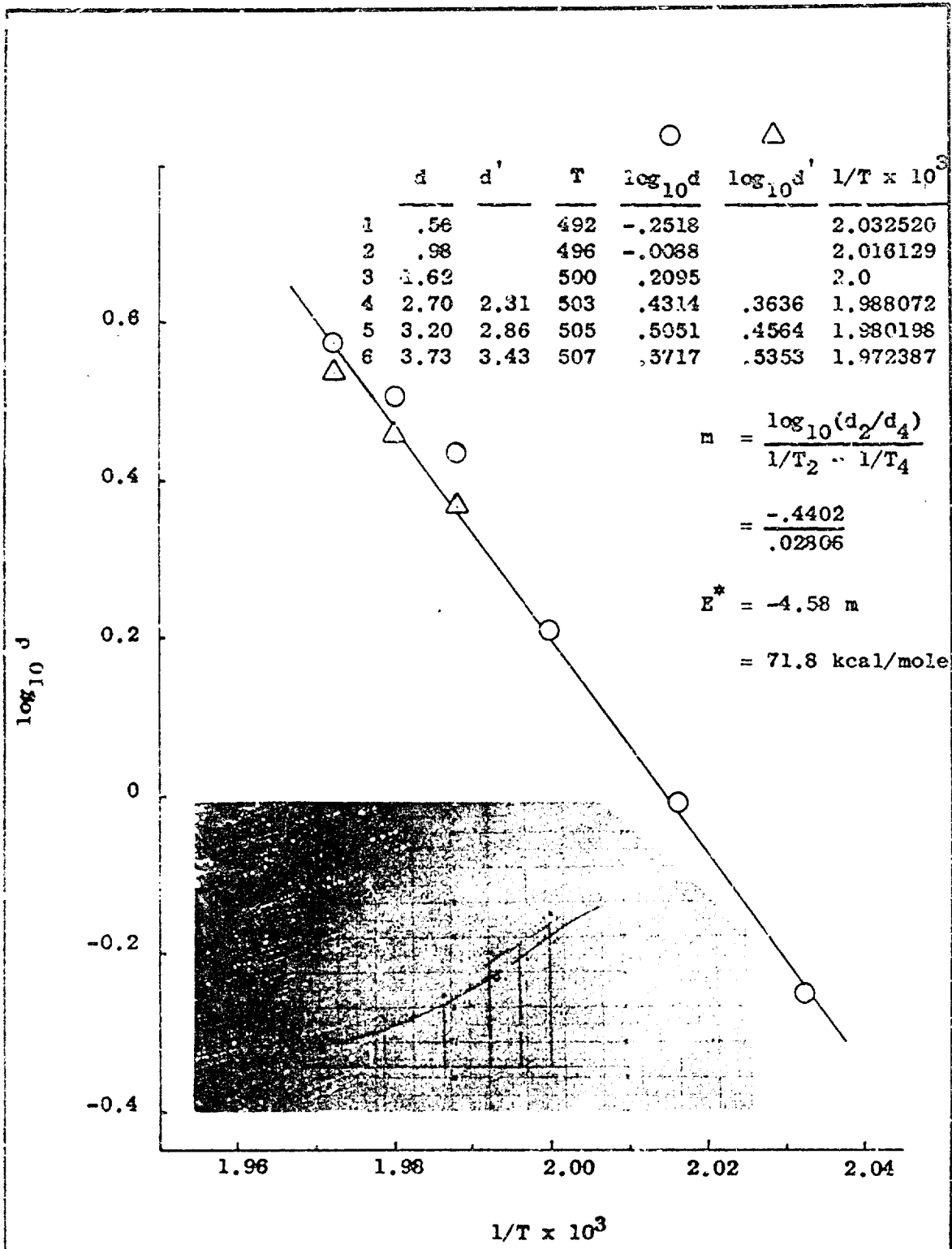


Figure D-5

Activation Energy: RDE (1) With Data Adjustment

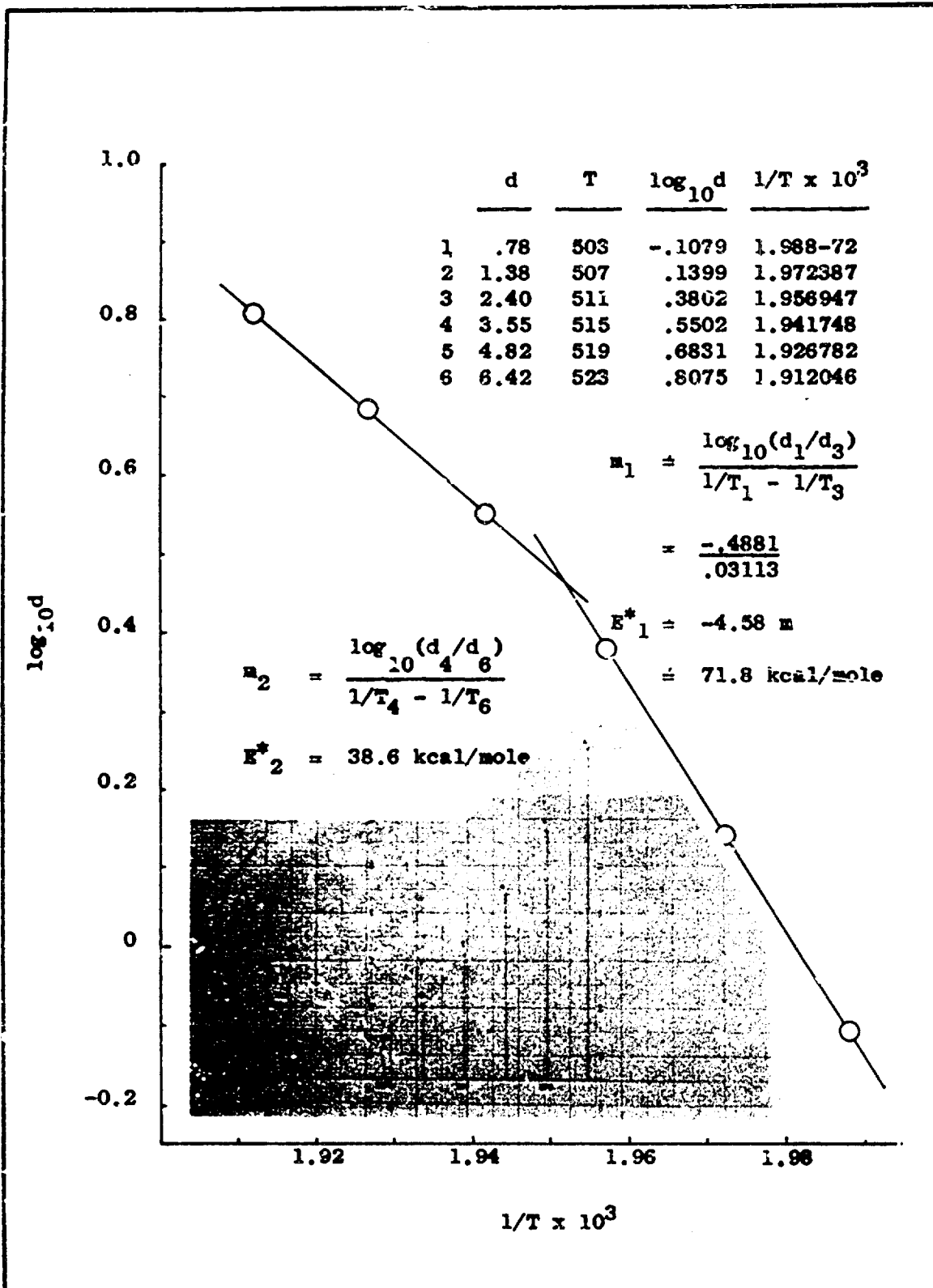


Figure D-6

Activation Energy: RDX (2) With Two Slopes

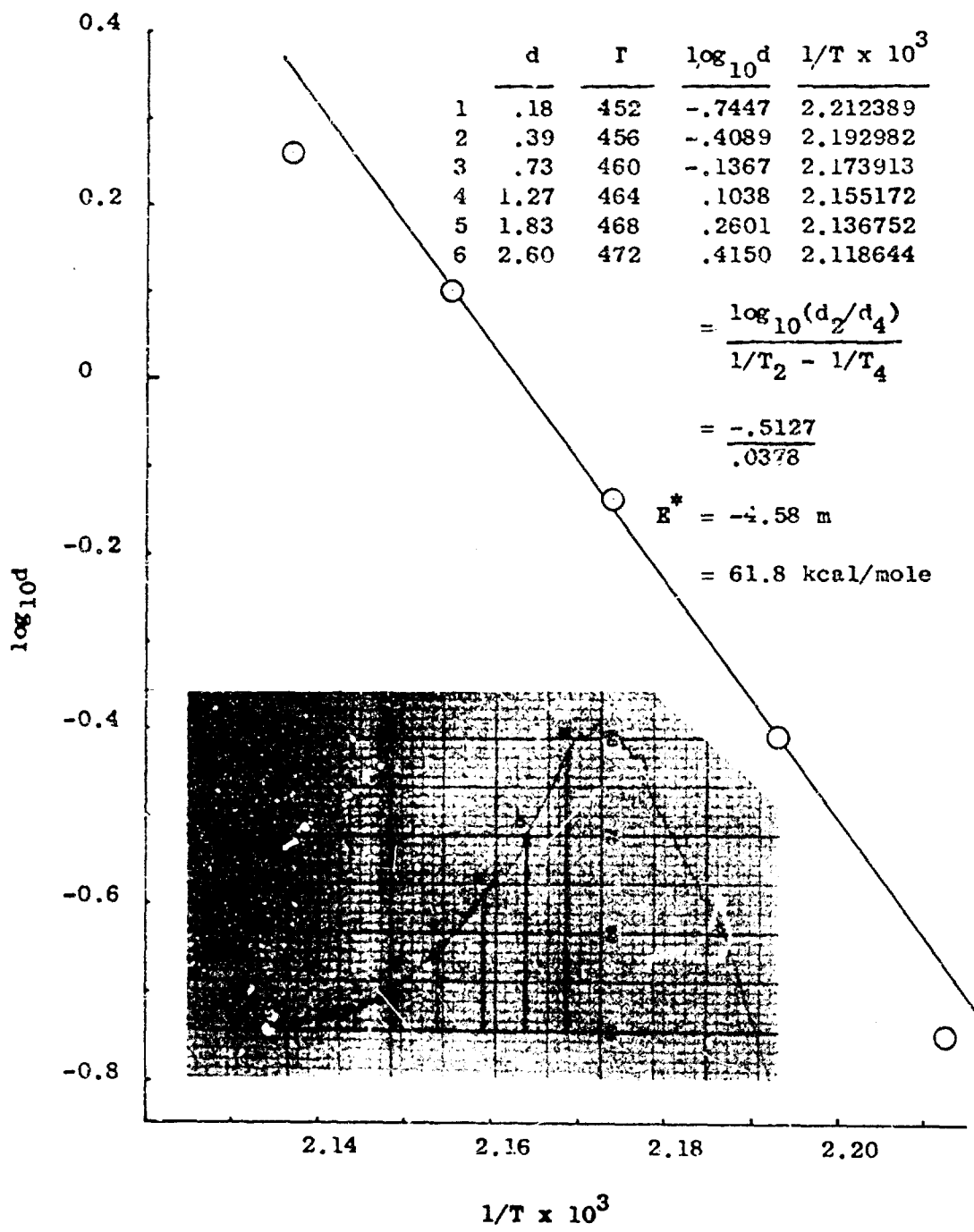


Figure D-7

Activation Energy: PETN (1)

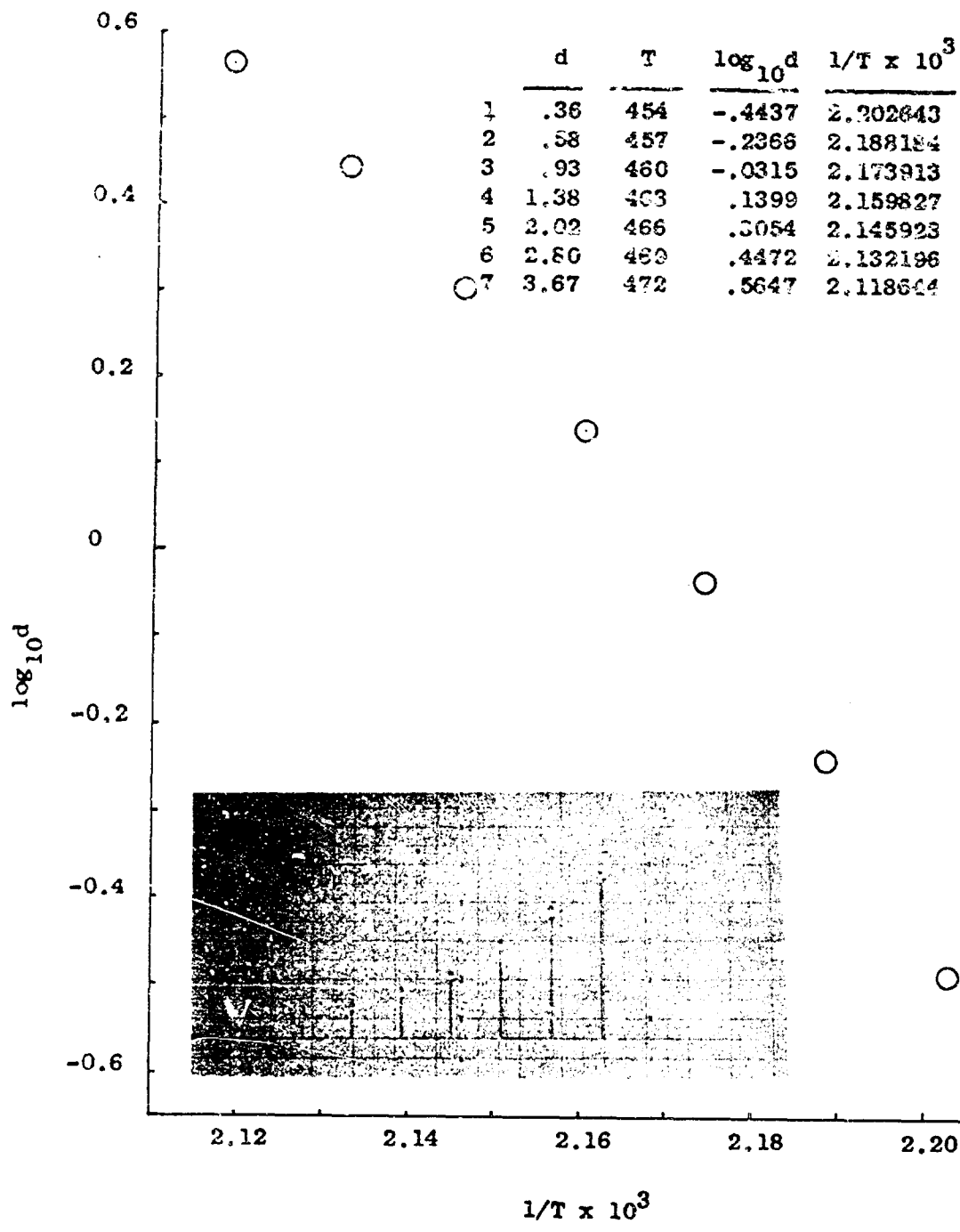


Figure D-8

Activation Energy: PETN (2) No Linearity

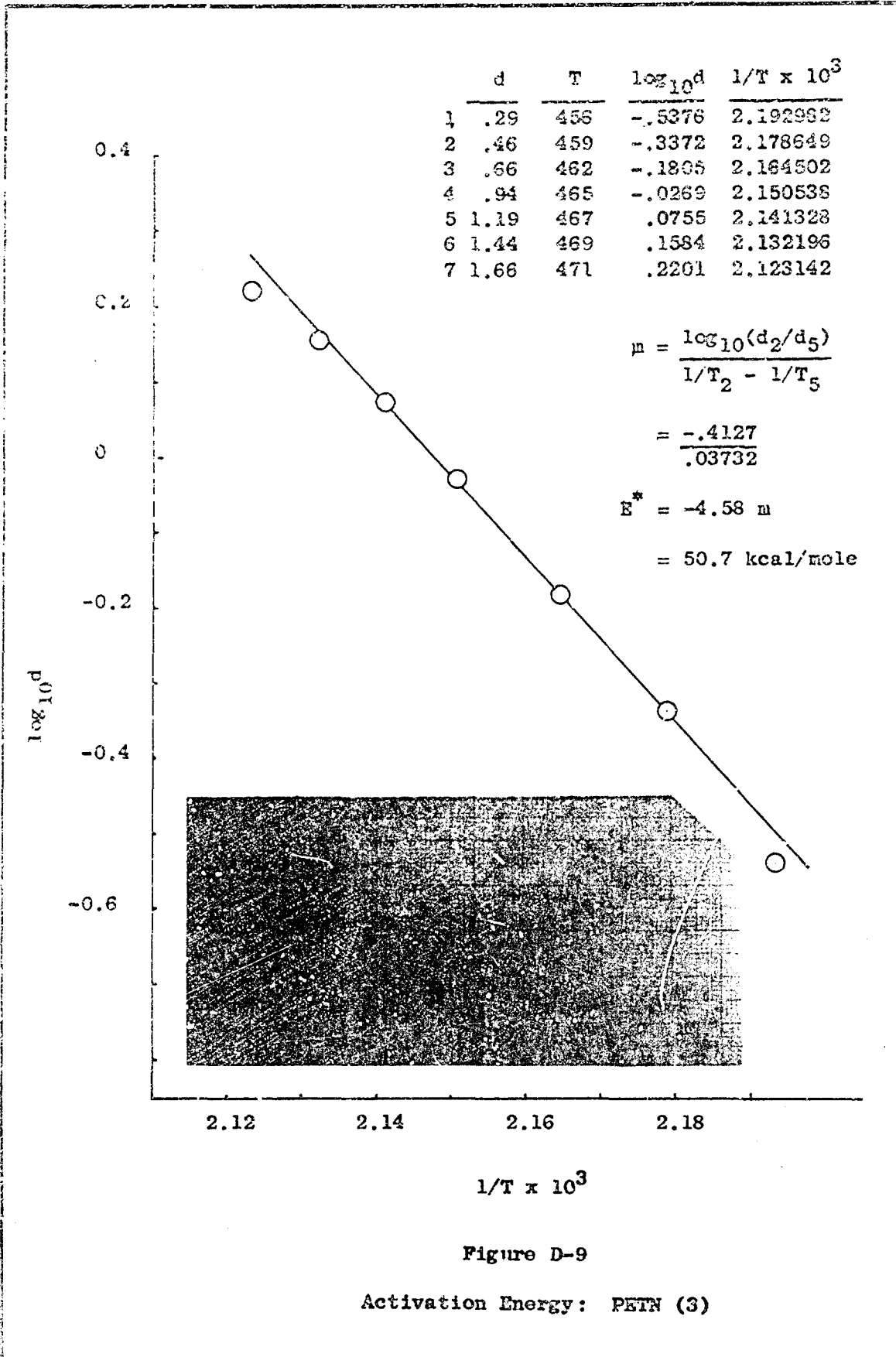


Figure D-9

Activation Energy: PETN (3)

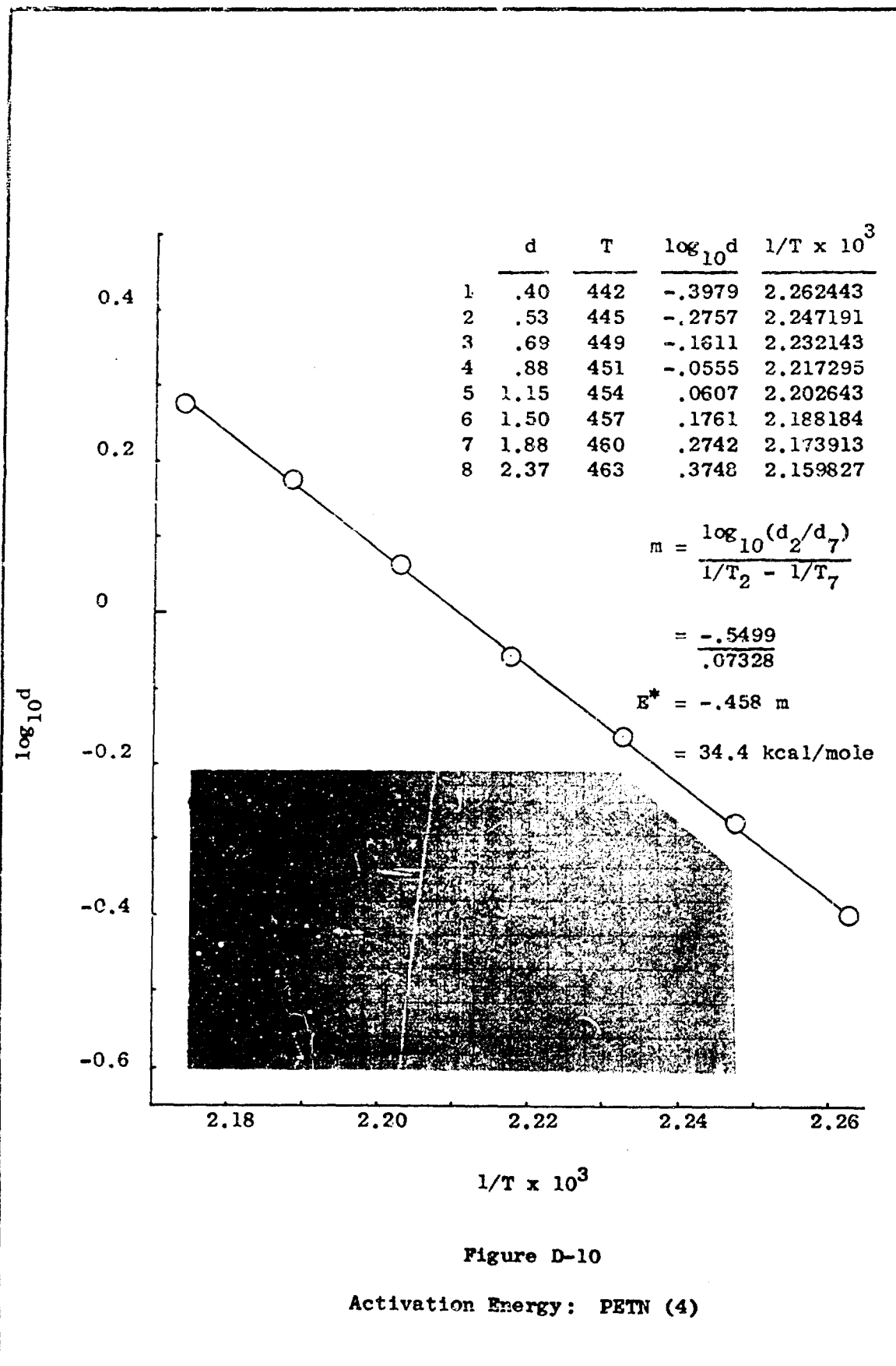


Figure D-10

Activation Energy: PETN (4)

Appendix E

Sources of Explosives

The explosives used in this study were obtained from the following sources:

- (1) Distillation Products Industries,
Rochester 3, New York
(Division of Eastman Kodak Company)
25 grams each

TNR and TNT No lot numbers
 No purity information

- (2) Lawrence Radiation Laboratories,
Livermore, California (Ref 17)
100 grams each

Tetryl (EK3047) Stock on hand over five years;
 Purity: no information

HMX (Lot A436) Origin: Holston Defense Corporation,
 Kingsport, Tennessee
 Purity: 99.8%+

RDX (Lot A212) Origin: Holston Defense Corporation,
 Kingsport, Tennessee
 Purity: no information

PETN (Lot A356) Origin: Trojan Powder Company,
 Allentown, Pennsylvania
 Purity: 98%+

No attempts were made to purify the explosives prior to testing.

Appendix F

Development of Purity Analysis

For an absolutely pure compound, the ordinary heat capacity dq/dT_s of the sample would approach infinity at the pure melting point T_o . But for an impure material, dq/dT_s is a function of sample temperature so that

$$dq/dT_s = q (T_o - T_m)/(T_o - T_s)^2 \quad (8)$$

The melting point depression due to impurities is calculated by

$$T_o - T_m = \frac{R T_o^2 X}{H_f} \quad (9)$$

Now, the fraction F of sample melted at any temperature T_s is

$$F = \frac{T_o - T_m}{T_o - T_s} \quad (10)$$

or

$$T_o - T_s = (T_o - T_m)(1/F) \quad (11)$$

which gives the slope-intercept equation for a straight line:

$$T_s = T_o - (T_o - T_m)(1/F) \quad (12)$$

Thus, with Equation (9)

$$\text{slope } m = T_o - T_m \quad (13)$$

$$= \frac{R T_o^2 X}{H_f} \quad (14)$$

where X is the mole fraction of impurity present. Therefore,

$$X = \frac{m H_f}{R T_o^2} \quad (4)$$

Appendix G

Development of Activation Energy Analysis

The basis for the development of the activation energy analysis is the Arrhenius equation, usually given in the form

$$k = A^* \exp(-E^*/RT) \quad (15)$$

For an explosive sample, the DSC trace deflections d_i along the decomposition exotherm are proportional to the Arrhenius rate constant k :

$$k = C d = A^* \exp(-E^*/RT) \quad (16)$$

which becomes

$$\ln C + \ln d = \ln A^* - E^*/RT \quad (17)$$

Any two points, (d_1, T_1) and (d_2, T_2) , are chosen: then

$$\ln C + \ln d_1 = \ln A^* - E^*/RT_1 \quad (18)$$

$$\ln C + \ln d_2 = \ln A^* - E^*/RT_2 \quad (19)$$

Subtracting, the constants C and A vanish:

$$\ln d_1 - \ln d_2 = -E^*/R (1/T_1 - 1/T_2) \quad (20)$$

or

$$-E^*/R = (\ln d_1 - \ln d_2)(1/T_1 - 1/T_2)^{-1} \quad (21)$$

$$= \frac{2.303 (\log_{10} d_1 - \log_{10} d_2)}{1/T_1 - 1/T_2} \quad (6)$$

For $R = 1.987$ kcal/mole $^{\circ}K$,

$$E^* = \frac{-4.58 \log_{10}(d_1/d_2)}{1/T_1 - 1/T_2} \quad (7)$$

Vita

Jerry Dean Wilcox was born on 21 May 1938 in Twin Falls, Idaho, the son of LeRoy Clark Wilcox and Letha Linford Wilcox. After completing his work in 1956 at Misawa American Dependent School, Crawford Branch, at Makomanai, Hokkaido, Japan, he enrolled at Brigham Young University and participated in the Air Force ROTC program. His schooling was interrupted for a three-year assignment as a Mormon missionary in Japan, after which he returned and graduated from Brigham Young University in June 1965 with a Bachelor of Engineering Science Degree in Mechanical Engineering and a commission as Lieutenant, United States Air Force. He entered active duty in August, 1965, at the Air Force Institute of Technology, Wright-Patterson Air Force Base, Ohio. He is a member of Tau Beta Pi, and is an Engineer in Training in the State of Utah.

Permanent address: 330 East 3200 North
Provo, Utah 84601

This thesis was typed by Mrs. Judy A. Fauver.

THIS DOCUMENT IS SUBJECT TO SPECIAL EXPORT
CONTROLS AND EACH TRANSMITTAL TO FOREIGN
GOVERNMENTS OR FOREIGN NATIONALS MAY BE
MADE ONLY WITH PRIOR APPROVAL OF THE DEAN,
SCHOOL OF ENGINEERING, (AFIT-SE),
WRIGHT-PATTERSON AIR FORCE BASE, OHIO 45433.

DOCUMENT CONTROL DATA - R & D

(Security classification of title, body of abstract and indexing annotation must be entered when the overall report is classified)

1. ORIGINATING ACTIVITY (Corporate author) Air Force Institute of Technology (AFIT-SE) Wright-Patterson AFB, Ohio		2a. REPORT SECURITY CLASSIFICATION UNCLASSIFIED	
		2b. GROUP	
3. REPORT TITLE Differential Scanning Calorimetry Methods in the Determination of Thermal Properties of Explosives			
4. DESCRIPTIVE NOTES (Type of report and inclusive dates) AFIT Thesis			
5. AUTHOR(S) (First name, middle initial, last name) Wilcox, Jerry D., Lieutenant, USAF			
6. REPORT DATE June 1967		7a. TOTAL NO. OF PAGES 70	7b. NO. OF REFS 39
8a. CONTRACT OR GRANT NO. N/A		9a. ORIGINATOR'S REPORT NUMBER(S) AFIT Thesis GAW/ME/67B-3	
b. PROJECT NO. N/A		9b. OTHER REPORT NO(S) (Any other numbers that may be assigned this report) N/A	
c.			
d.			
10. DISTRIBUTION STATEMENT 			
11. SUPPLEMENTARY NOTES		12. SPONSORING MILITARY ACTIVITY	
13. ABSTRACT <p>Differential Scanning Calorimetry methods are applied in determining heat of fusion, purity, specific heat, and activation energy of decomposition for undiluted, unmixed samples of the high explosives TNR, TNT, tetryl, HMX, RDX, and PETN. Thermograms describing energy absorption or evolution from 300°K to 600°K are presented. Heat of fusion and purity results are consistent for explosives which melt at lower temperatures without vaporization, such as TNT and tetryl. Specific heat values in the 313°K to 423°K range all lie between 0.25 and 0.35 cal/gm °K, monotonically increasing with temperature. Activation energies obtained are 20% to 50% higher than those reported from isothermal tests.</p>			

14.

KEY WORDS

LINK A

LINK B

LINK C

ROLE

WT

ROLE

WT

ROLE

WT

Differential Scanning Calorimetry
Differential Thermal Analysis
Explosives
Properties of Explosives
Activation Energy of Decomposition
Specific Heat